Fall 2021

An Investigation of the Ignition Propensities of Fuels Perturbed by Nitrogen Monoxide

Ackmer Robinson III

An Investigation of the Ignition Propensities of Fuels Perturbed by Nitrogen Monoxide

By

Ackmer Robinson III

Bachelor of Science
University of South Carolina, 2019

Submitted in Partial Fulfillment of the Requirements

For the Degree of Master of Science in

Mechanical Engineering

College of Engineering and Computing

University of South Carolina

2021

Accepted by:

Sang Hee Won, Director of Thesis

Tanvir Farouk, Reader

Tracey L. Weldon, Interim Vice Provost and Dean of the Graduate School

ACKNOWLEDGEMENTS

I would like to acknowledge my advisor Dr. Sang Hee Won for his guidance and wisdom throughout the research process. I would also like to acknowledge The University of South Carolina for providing the necessary resources for the work done in this thesis.

ABSTRACT

Quantitative structure property relationship (QSPR) regression models were developed based on the chemical functional group distribution of toluene reference fuels (TRF, mixtures of n-heptane, iso-octane, and toluene) for RON, MON, and DCN. The QSPR regression models were developed using DCN measurements from this study as well as RON/MON data available in literature. The correlations between RON/MON and DCN were analyzed. The ignition propensity of TRFs perturbed by NO addition was also investigated in this study. The interactions between the chemical functional groups and NO were investigated using an ignition quality tester (IQT). It was found that the increase in the ignition propensity of TRFs after NO perturbation was directly related to the mole fraction of the $(CH_2)_n$ chemical functional group present in the TRFs. The chemical functional group distributions of an ethanol free gasoline with an AKI of 89 and five distillation cuts of the gasoline were determined using Nuclear magnetic resonance (NMR). The NMR analysis suggests that the mole fraction of the $(CH_2)_n$ functional group decreases from the lighter end of the distillation cuts to the heavier end of the distillation cuts. The current research suggests that the autoignition associated with knock and low speed pre-ignition (LSPI) in internal combustion engines may be caused by the interactions between NO, either left in the cylinder from the previous cycle or introduced by exhaust gas recirculation, and the $(CH_2)_n$ functional group in gasoline.

TABLE OF CONTENTS

LIST OF TABLES

LIST OF FIGURES

LIST OF SYMBOLS

NO_{ppm}	Parts per million of nitrogen monoxide
P_{N_2}	Partial pressure of nitrogen
P_{NO/N_2}	Partial pressure of nitrogen monoxide and nitrogen mixture
P_{O_2}	Partial pressure of oxygen
P_t	Total pressure

LIST OF ABREVIATIONS

AKI ..... Anti-knock index

CFR ..... Cooperative Fuel Research

CI ..... Compression Ignition

CN ..... Cetane number

CPT ..... Combustion property targets

DCN ..... Derived cetane number

GDI ..... Gasoline direct injection

HCCI ..... Homogeneous charge compression ignition

H/C ratio ..... Hydrogen to Carbon ratio

IDT ..... Ignition delay time

IQT ..... Ignition Quality Tester

LSPI ..... Low speed pre-ignition

MON ..... Motor octane number

MW ..... Molecular weight

NMR ..... Nuclear magnetic resonance

PRF ..... Primary reference fuels

QSPR..... Quantitative structure property relationship

RON ..... Research octane number

SI ..... Spark ignition

TRF ..... Toluene reference fuels

TSI..... Threshold sooting index

CHAPTER 1

INTRODUCTION

Energy is one of the most in demand products of our modern world and the demand for energy is projected to increase for the foreseeable future. As more countries develop their economies, the need for energy will become more prevalent. For this reason, it is necessary to develop systems that efficiently produce energy without causing harmful environmental effects. Many strides have been made with renewable energy sources, however, most of the energy in use today is produced by burning fossil fuels. Fossil fuels are produced by refining crude oil that is mined from the earth. Some examples of fossil fuels are coal, petroleum, and natural gas. These fuels are burned in engines that allow the chemical enthalpy of the fuels to be converted into mechanical energy that can be used to do work. Although the goal is to shift away from using fossil fuels for energy production, due to the harsh environmental effects, the shift away from fossil fuels for energy production will likely take many years and many advancements in technology. At the current time it is of importance to maximize the efficiency and minimize the emissions of engines burning fossil fuels so that the harmful environmental effects can be minimized until new technologies emerge that allow for energy production without the use of fossil fuels.

In the United States there have been major changes in the way energy has been produced over the last 200 years. In the early 1800s most of the energy consumed in the

U.S. was produced by burning wood as can be seen in **Fig. 1.1** below. Towards the end of the 19th century there was a shift from energy production by wood to energy production by fossil fuels such as coal, petroleum, and natural gas. Over the last century energy production in the U.S. has had a more significant contribution from hydroelectric, nuclear, and other renewable energy sources. An energy source is considered renewable if the source is naturally replenishing but restricted by the amount of energy that is available per unit time [1]. In 2020 there was a major increase in the amount of energy produced by renewable energy sources. Renewable energy provided around 12% of the total U.S. energy consumption in 2020 [1]. The shift toward more energy production by renewable energy sources is ideal, however, the amount of energy that can be produced by renewable sources alone cannot currently meet energy demands. For this reason, it is of great importance to optimize energy production using fossil fuels until a time comes when renewable energy sources can meet energy demands.

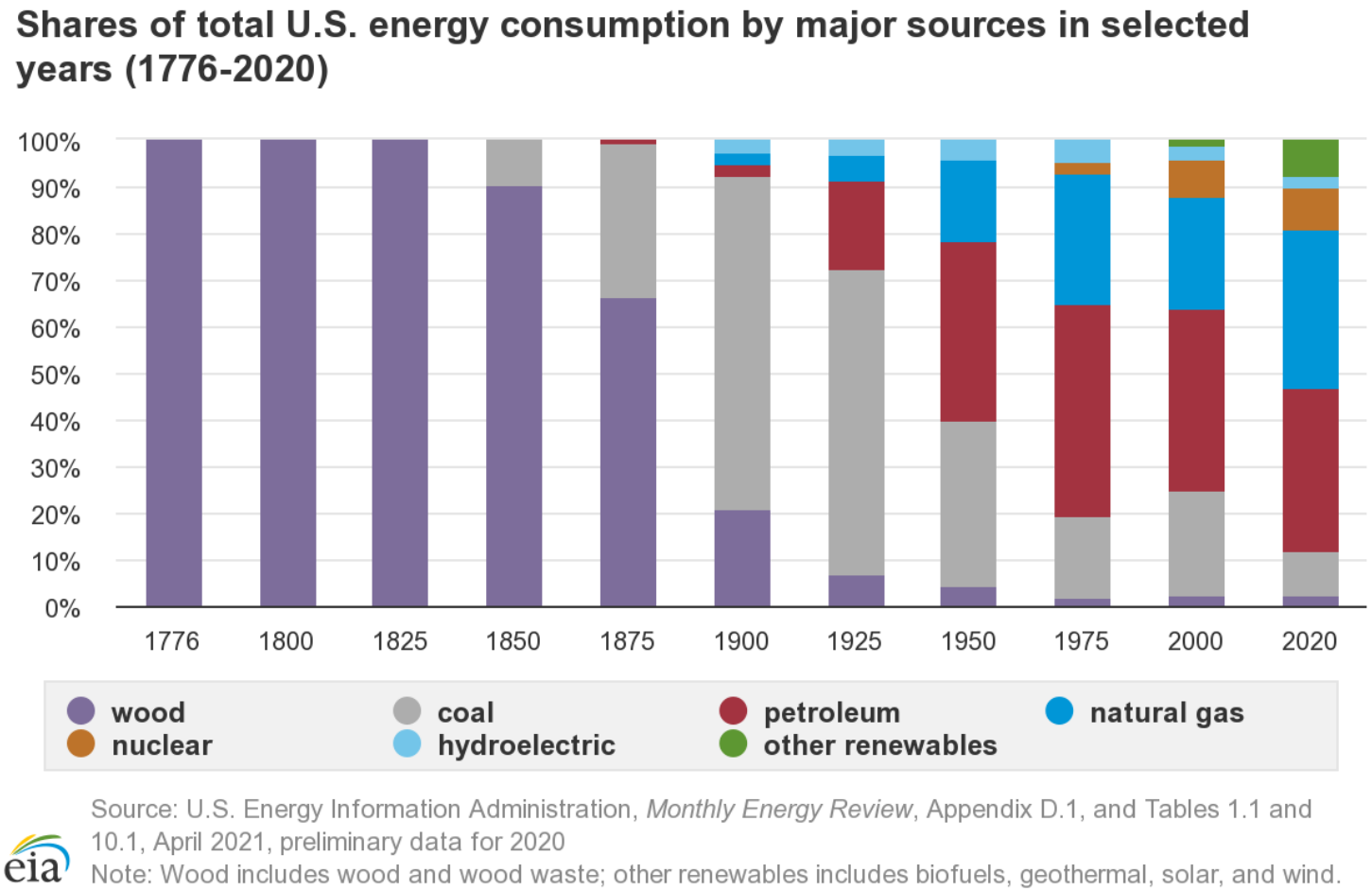

Figure 1.1. Shares of total U.S. energy consumption by major sources in selected years (1776 – 2020).

The energy that is produced in the U.S., as well as the energy consumed, comes from many different sources. In the U.S. primary energy consumption, or energy consumed by fossil fuels, nuclear, and renewable sources, was equal to nearly 93 quadrillion Btu in 2020 [2]. **Figure 1.2** shows the distribution of U.S. primary energy consumption by energy source in 2020. It can be observed from **Fig. 1.2** that most of the energy consumption in the U.S. is produced by fossil fuels (petroleum, natural gas, and coal). Other energy sources only make up about 21% of the total energy consumption in the U.S. **Figure 1.3** shows the contribution of different energy sources to primary energy consumption in the U.S. with respects to time. Since 1950 energy consumption in the U.S. has increased drastically. Energy consumption by nuclear and renewable energy sources have been increasing over time, but most of the energy consumed in the U.S. over the last 70 years has been produced by fossil fuels. Energy production in the U.S. has followed similar trends to the energy consumption in the U.S. since 1950. **Figure 1.4** shows the contribution of different energy sources to primary energy production in the U.S. There has been a major increase in the amount of energy produced by the U.S. since 1950 with the maximum energy produced in the U.S. taking place in 2019. **Figure 1.5** shows the primary energy production in the U.S. by different energy sources in 2020. Most of the energy produced in 2020 in the U.S. was by fossil fuels (nearly 70 %). The energy consumption and production trends in the U.S. over the past 200 years show the significance of fossil fuels in our modern world and why it is important to efficiently burn fossil fuels when producing energy.

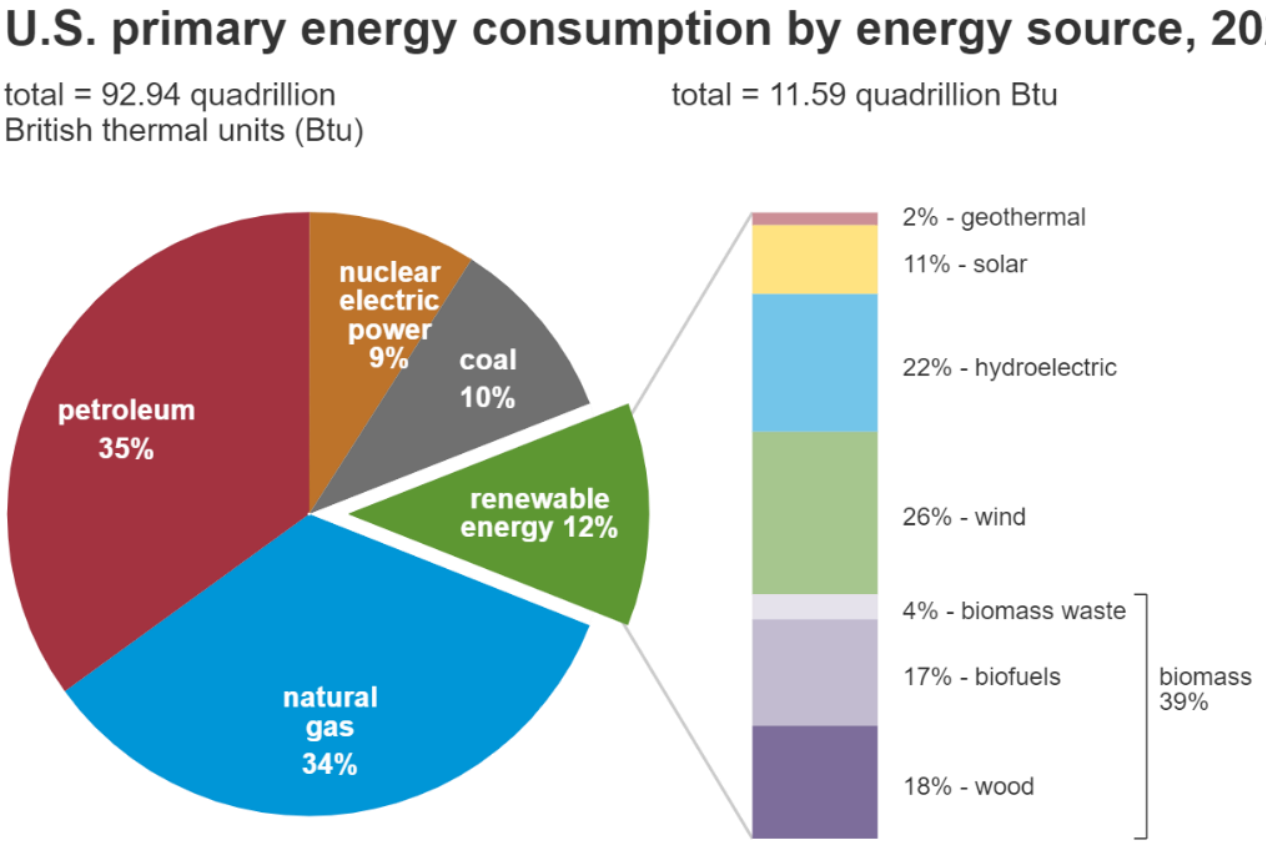

Source: U.S. Energy Information Administration, *Monthly Energy Review*, Table 1.3 and 10.1, April 2021, preliminary data
Note: Sum of components may not equal 100% because of independent rounding.

Figure 1.2. U.S. primary energy consumption by energy source, 2020.

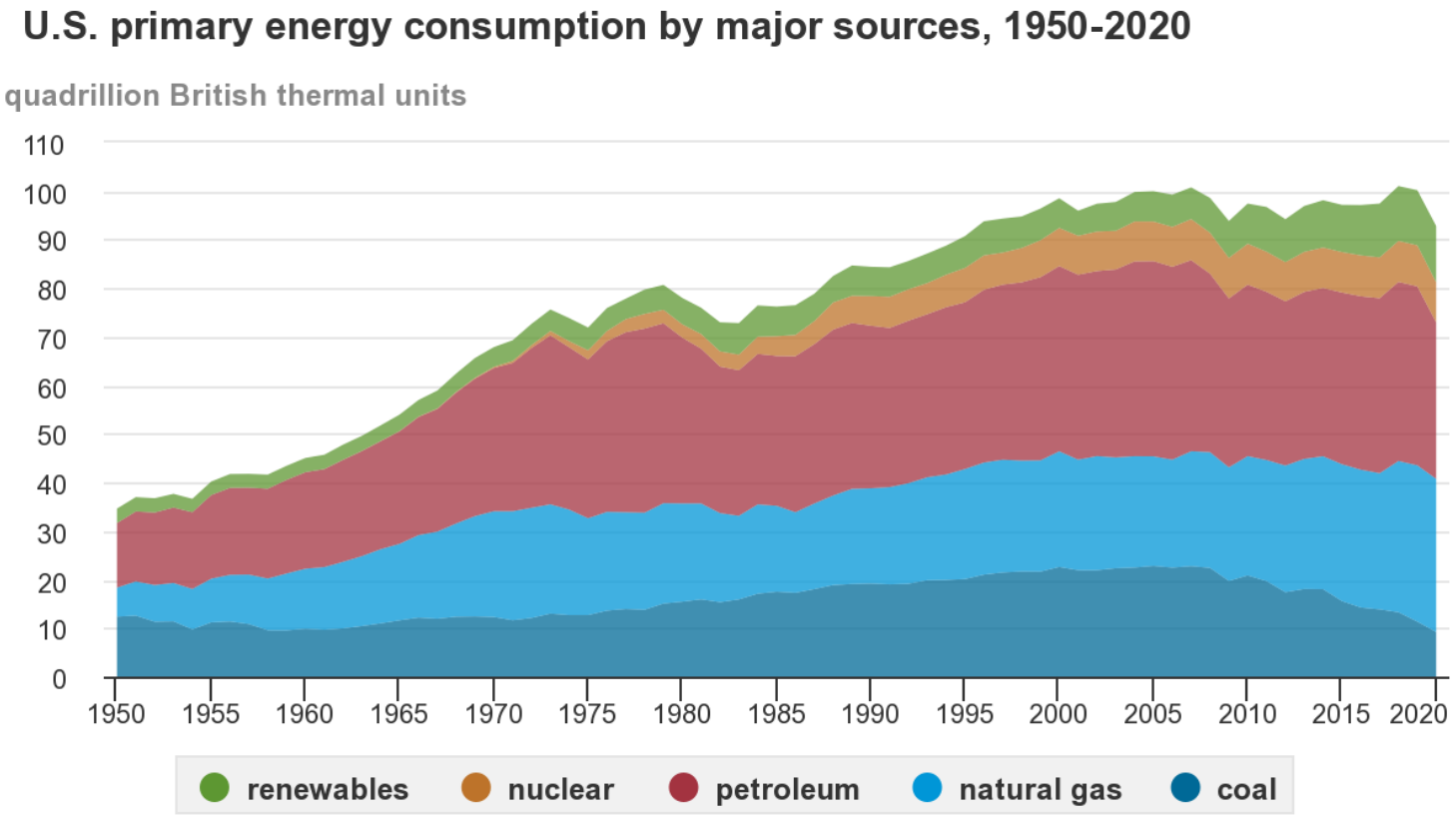

Figure 1.3. U.S. primary energy consumption by major sources, 1950-2020.

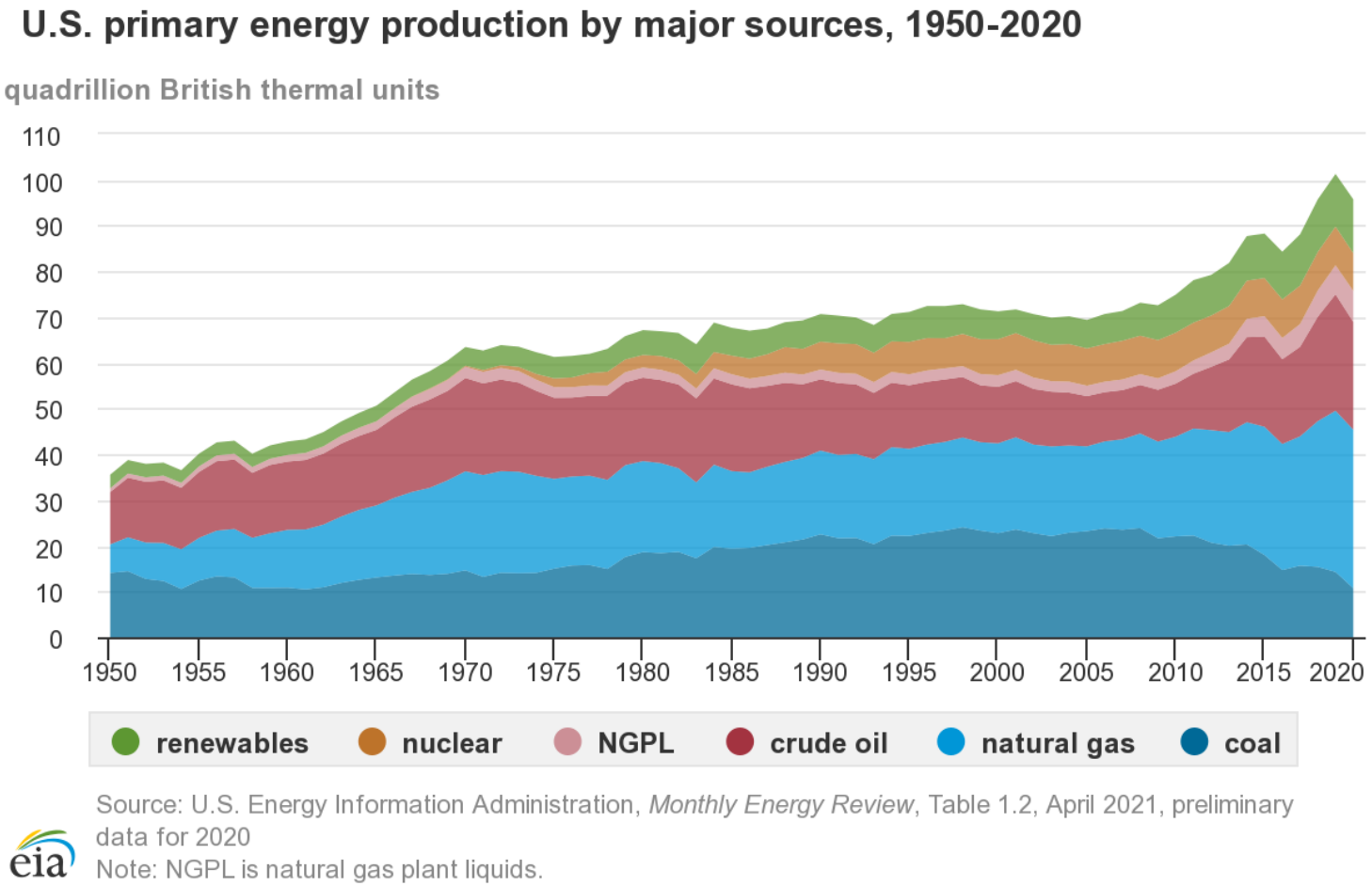

Figure 1.4. U.S. primary energy production by major sources, 1950-2020.

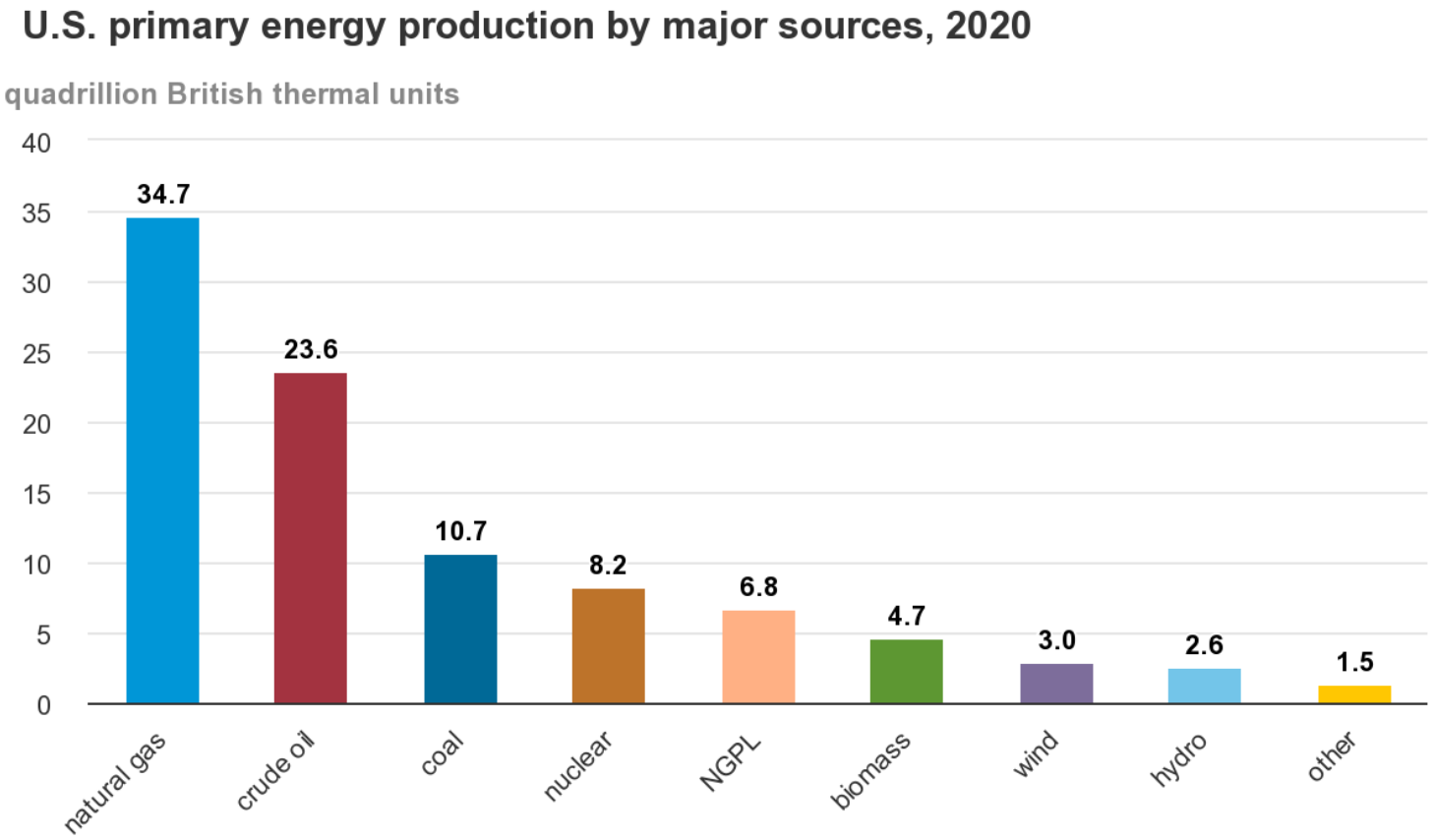

Figure 1.5. U.S. primary energy production by major sources, 2020.

Petroleum is the major contributor to energy production for the transportation sector and provided nearly 90% of the transportation sector's energy consumption in 2020 [2]. The transportation sector includes land vehicles, such as cars and trucks, marine vehicles, and aerial vehicles. Most land vehicles utilize internal combustion engines that convert the chemical enthalpy of fuel to mechanical energy that can be used to do work. Internal combustion engines have been used to produce mechanical energy for many years. The two main types of internal combustion engines are compression ignition engines and spark ignition engines. Compression ignition engines usually burn diesel fuel and do not require an ignition source for the combustion process to initiate. Compression ignition engines rely on the high pressure and the high temperature conditions in the combustion chamber to initiate the combustion process. Spark ignition engines on the other hand usually burn gasoline and are dependent on an ignition source. In a spark ignition engine, the combustion of a mixture of fuel and air at high temperature and pressure is initiated by an ignition source such as a spark plug.

Internal combustion engines burn mixtures of fuel and air at high temperature and high pressure. The quality of fuels burned in internal combustion engines is quantified by different methods depending on the fuel being burned. The cetane number (CN) is used to quantify the quality of diesel fuels. The CN is a way to measure how well the diesel fuel ignites at given temperature and pressure specifications. For gasoline fuels there are many quantities used to describe the quality of fuel. Two of the main quantities used to describe the quality of gasoline fuel are the research octane number (RON) and the motor octane number (MON). Sometimes the RON and MON are averaged to determine another quantity called the anti-knock index (AKI). The RON, MON, and AKI are all

quantities used to determine how well a fuel resist engine knock. Knock is a phenomenon that occurs in spark ignition engines when ignition occurs in the fuel and air mixture before the spark ignitor has a chance to ignite the mixture. When ignition occurs automatically before the spark igniter has a chance to ignite the fuel it is called autoignition. Engine knock is detrimental to engine timing and can cause major engine damage if the effects are significant.

Since the initial development of internal combustion engines, many advancements have been made to improve the performance of these engines. Some of the major contributions to the improved performance of internal combustion engines are the development of boosting technologies as well as the emergence of exhaust gas recirculation. Introducing the recirculated exhaust gases of an internal combustion engine into the incoming airstream of the engine allows for the incoming air to be heated by the temperature of the exhaust gas and allows the unburned fuel remaining in the exhaust gas to be burned [3]. These effects lead to better thermal efficiency and reduced emissions. Some of the emissions related to internal combustion engines are unburned hydrocarbons (UHC), oxides of nitrogen (NO_x), oxides of sulfur (SO_x), carbon monoxide (CO), and carbon dioxide (CO_2).

Real petroleum-derived fuels, such as gasoline and diesel, are composed of many complex chemical mixtures with complicated molecular structures. The complexity of the chemical structures in real fuels makes it difficult to design chemical kinetic models that accurately predict the combustion behavior of real fuels. Some progress has been made to reduce the chemical kinetic models used to represent the complex chemical mechanisms of real fuels, however, more experimental data is still needed to verify that the reduced

chemical kinetic models can accurately predict combustion behavior [4]. The complexity of petroleum-derived fuels makes modeling the fuels difficult, but it has been found in previous studies [5-7], that the combustion behavior of real fuels can be predicted by using surrogate fuels with similar combustion property targets (CPTs), such as hydrogen to carbon ratio (H/C ratio), threshold sooting index (TSI), derived cetane number (DCN), molecular weight (MW), and chemical functional group distribution, as the real petroleum-derived fuels.

The objectives of the current research are to interpret the role(s) of RON and MON through chemical functional group analysis, relate RON and MON to DCN through chemical functional group descriptors, and investigate the role(s) of nitrogen monoxide, NO, addition on ignition propensity of toluene reference fuels (TRFs, mixtures of n-heptane, iso-octane, and toluene) through DCN measurements. TRFs were chosen, based on their chemical functional group distributions, to represent real fuels. TRFs have been used in previous studies to model gasoline and to develop chemical kinetic models to predict the combustion behavior of real fuels (e.g. [8]). Chemical functional groups are fragments of molecules that behave in similar ways throughout the combustion process regardless of the molecule that they are attached to. If the distribution of the chemical functional groups in a fuel mixture is known, then the combustion behavior of the fuel mixture can be predicted. Quantitative structure property relationship (QSPR) regression models were developed using Scheffé polynomials for RON, MON, and DCN based on data in the literature [8] and data from the DCN measurements of the current research. The developed QSPR regression models are then used to relate the RON and MON to DCN through the chemical functional group descriptors. An ignition quality

tester (IQT) was used to better understand the effects of nitrogen monoxide, NO, on the ignition propensity of TRFs and the role(s) NO plays in the chemical kinetics of the combustion process.

CHAPTER 2

THEORY

The chemical complexity of real petroleum derived fuels, such as gasoline, jet fuels, and diesel, can make modeling difficult. Real petroleum derived fuels are composed of hundreds and sometimes thousands of molecules with a large variety of molecular structures. Most of the molecular structures found in petroleum derived fuels are hydrocarbons. Though hydrocarbons are all composed of hydrogen and carbon atoms, there can be large differences in how these atoms combine to make molecules. The differences in the molecular structures of molecules can vastly change the chemical roles the molecules play in the combustion process even if the molecules are composed of the same atoms. For this reason, families of hydrocarbons were developed based on the molecular structure of the hydrocarbon molecules.

There are five major families used to categorize hydrocarbons based on their molecular structures. The five hydrocarbon families are alkanes, alkenes, alkynes, cycloalkanes, and aromatics (benzyl-type structures). Each family is defined based on how the hydrogen and carbon atoms are arranged in the molecular structure. Alkanes are hydrocarbon molecules that have an open-chain structure and contain only one bond between all carbon atoms in the molecule. Alkanes can be divided further into two categories depending on how the molecule is arranged. n-Alkanes, such as n-heptane, are linear alkanes meaning that all the carbon atoms in the molecule are connected linearly.

Branched chain alkanes, also known as iso-alkanes, are alkanes where some of the carbon atoms in the molecule are not linearly connected. Two alkane molecules such as n-heptane and iso-heptane (2-methyl hexane) can have the same generic chemical formula (C_7H_{16}) but major differences in molecular structure and chemical behavior. Alkenes are hydrocarbon molecules that have an open-chain structure and contain at least one double bond between two carbon atoms in the molecule. Alkynes are hydrocarbon molecules that have an open-chain structure and contain at least one triple bond between two carbon atoms in the molecule. Cycloalkanes are hydrocarbon molecules that have closed ring structures and contain only one bond between all carbon atoms in the molecule and aromatics are hydrocarbon molecules that have closed ring structures and contain aromatic bonds (e.g., the benzene molecule).

Real petroleum derived fuels are complex mixtures of mostly n-alkanes, iso-alkanes, cycloalkanes, and aromatics. The differences in molecular structure cause differences in overall combustion behavior. The chemical complexity of real fuels makes it difficult to construct models that can predict the combustion behavior of the fuels. There are hundreds and sometimes even thousands of chemical components that make up a real fuel and it is nearly impossible to construct models that can accurately represent the combustion pathways of each of the individual chemical components. To simplify chemical kinetic models without losing the fidelity of the overall combustion behavior surrogate mixtures can be used. Surrogate mixtures are mixtures of one or more known chemical components used to model the chemical behavior of a real fuel. The objective when developing a surrogate fuel is to match the chemical behavior of a real fuel while using as few chemical components as possible. There are many methods used to choose

surrogate mixtures however most of the time the surrogate mixture determination depends on what is being studied and how accurately the surrogate mixture should match the real fuel.

Internal combustion engines typically burn gasoline or diesel. Gasoline is usually burned in spark ignition (SI) engines whereas diesel is usually burned in compression ignition (CI) engines. In SI engines a fuel and air mixture at high temperature and pressure is ignited by an ignition source such as a spark plug. In CI engines the ignition is initiated by the fuel injection at relatively high chamber temperature due to rapid compression of air. The quality of gasoline or diesel fuel is measured based on standardized test procedures. For gasoline, the quality of the fuel can be measured using the research octane number (RON) or the motor octane number (MON). The RON and MON fuel ratings were initially established in 1927 and are determined using the ASTM standard procedure in an SI CFR (Cooperative Fuel Research) F1/F2 engine [9]. The RON test procedure follows the ASTM D2699 standard, and the MON test procedure follows the ASTM D2700 standard. To determine the RON and MON of a given fuel, the fuel is tested in the CFR engine and compared to the values of RON and MON of primary reference fuels (PRFs, mixtures of n-heptane and iso-octane). For both RON and MON measurements iso-octane is given a RON and MON value of 100 and n-heptane is given a RON and MON value of 0. RON and MON are both experimentally determined measurements of the quality of fuel, but RON and MON are used to simulate engine performance under different conditions. RON is measured at an engine speed of 600 rpm and is used to simulate lower engine speeds and lower loads. MON is measured at an engine speed of 900 rpm and is used to simulate higher engine speeds and higher loads.

For diesel, the quality of the fuel can be measured using the cetane number (CN). The CN of a fuel can be determined in a similar way to that of the RON and MON. Cetane measurements are conducted in a CFR F5 engine and compared to reference fuels where cetane (n-hexadecane) and iso-cetane (2,2,4,4,6,8,8-heptamethylnonane) are used as references [9]. The derived cetane number (DCN) of a fuel can be measured using an ignition quality tester (IQT) in accordance with the ASTM D6890 testing procedure. **Figure 2.1** shows the IQT system. The IQT is a constant volume combustion chamber used to measure the ignition quality of distillate fuels. The IQT measures the ignition delay time (IDT) of a given fuel and then derives the cetane number from the measured IDT. The IDT is measured as the time between fuel injection and a pressure rise in the combustion chamber signifying ignition. **Figure 2.2** shows how the IDT is measured. The yellow curve indicates the injector displacement, and the blue curve indicates the combustion chamber pressure. The rapid change in injector displacement signifies the fuel injection and the rapid rise in chamber pressure indicates the ignition of the fuel and air mixture in the combustion chamber. Due to the differences in measurement procedures, the DCN measured by the IQT is different than the CN measured by the CFR F5 engine. The DCN and the CN are however comparable in values for a given fuel sample.

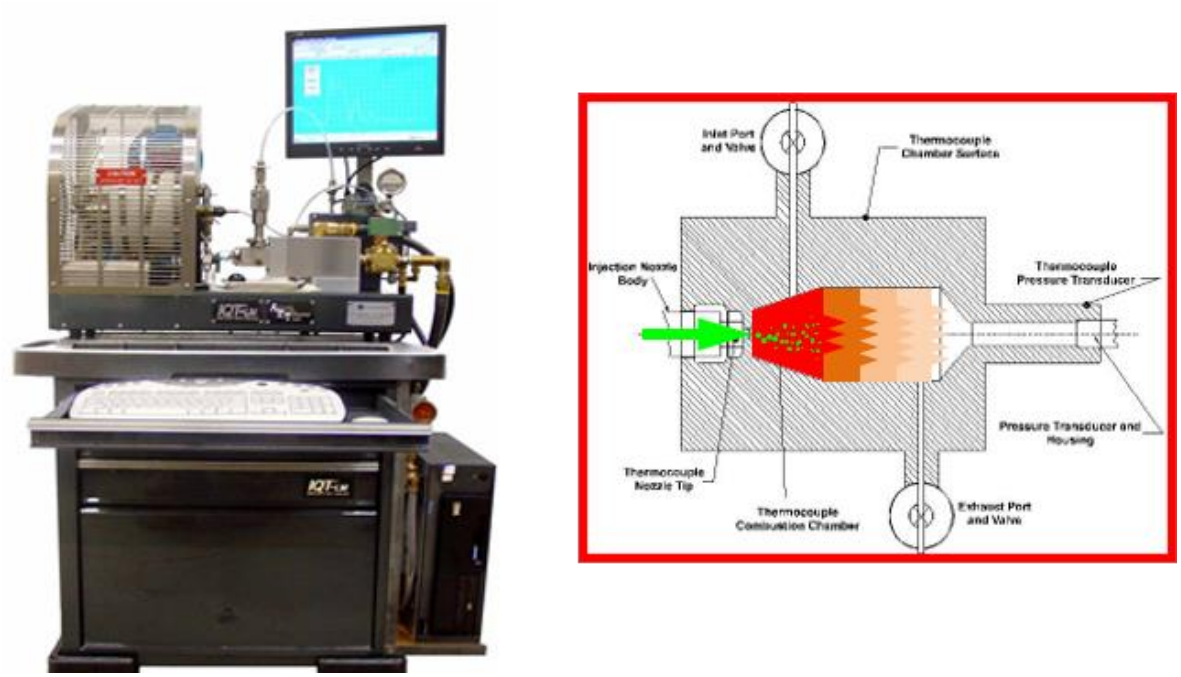

Figure 2.1. Ignition quality tester (IQT).

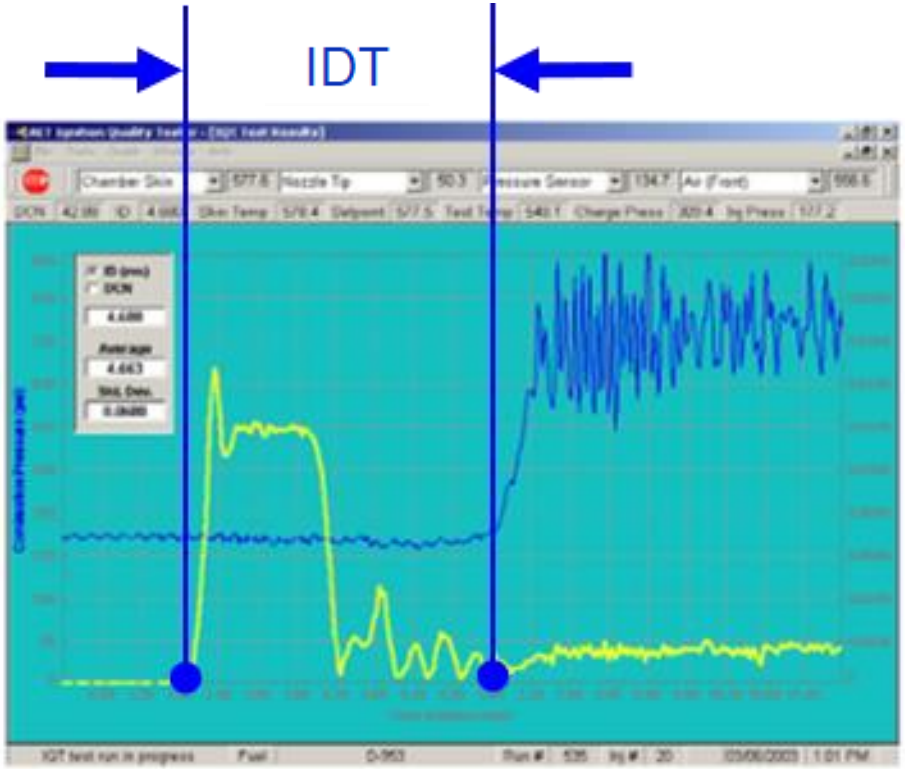

Figure 2.2. Ignition delay time (IDT).

The chemical complexity of real fuels can be reduced if the chemical functional group approach is used. The chemical functional group approach is a method used to break down the complex chemical mixtures of real fuels into small groups of atoms with the same chemical functionality. There are five key functional groups known to be relevant to overall combustion behavior. The five key functional groups are the linearly bonded methylene group ($(CH_2)_n$ where "n" indicates the resulting carbon chain length), the isolated methylene group (CH_2), the methyl group (CH_3), the cycloalkyl group $(CH_2)_{cyclo}$, and the benzyl-type functional group [7]. The $(CH_2)_n$ functional group can be found in n-alkanes and is known to promote reactivity through thermal decomposition or low-temperature chain branching reactions. The CH_2 functional group is known to have relatively weak bond energies. The CH_3 functional group can be found mostly in iso-alkanes and requires H-abstraction reactions. The $(CH_2)_{cyclo}$ functional group stems from cycloalkanes and for high temperature combustion has similar reactivities to n-alkanes. For low temperature combustion it is difficult for the $(CH_2)_{cyclo}$ functional group to initiate chain branching reactions. Lastly, the benzyl-type functional group stems from aromatics and is known to slow down overall reactivity. Two more functional groups that should also be mentioned are the CH functional group and the C functional group. The CH functional group and the C functional group are included in the chemical functional group analysis of the current research but, the CH functional group and the C functional group have less significant contributions to combustion behavior than the other functional groups. The chemical functional group approach can be utilized because the behavior of the functional groups is well known and has no significant change regardless of what molecule the chemical functional groups are attached to. This means that if the chemical

functional group distribution of a given fuel can be determined, then the combustion behavior of the fuel can be predicted based on the distribution of the chemical functional groups.

The chemical functional group distribution of a given fuel sample can be determined through nuclear magnetic resonance (NMR) spectroscopy. NMR spectroscopy is a tool used to detect the configuration of atoms in a molecule. Some atoms have nuclei with a nuclear spin and this nuclear spin generates an electromagnetic field. The intensity of the electromagnetic field generated by an atom's nuclei changes depending on how the atom is configured in a molecule. NMR spectroscopy takes advantage of this property of atomic nuclei. When NMR spectroscopy is performed a chemical sample is placed in a magnetic field. This magnetic field aligns the nuclei of the specific atoms with, or in the opposite direction of, the magnetic field. Once the atomic nuclei are aligned the sample is exposed to electromagnetic radiation at specific frequencies. If the electromagnetic radiation is tuned to the right frequency, known as the resonance frequency, then the atomic nuclei that are aligned with the magnetic field will absorb energy from the electromagnetic radiation and experience a "spin flip" where the atomic nuclei align in the opposite direction of the magnetic field [10]. The spin flip of the atomic nuclei at the resonance frequency is then detected by a detector. NMR spectra is plotted as a two-dimensional graph where the horizontal axis is the chemical shift, directly related to the electromagnetic radiation frequency, and the vertical axis is the intensity of the atomic nuclei's absorption. The chemical shift of an atomic nuclei is the position on the plot at which the nuclei absorb the electromagnetic radiation [10]. The chemical shift of an atomic nuclei is dependent on how the atom is arranged in the

molecule. If the chemical shifts of specific molecular configurations are known, then the distribution of the specific molecular configurations in a sample can be determined using NMR spectroscopy.

In recent years there has been a demand to downsize engines while maintaining engine performance. Downsized engines have been shown to have better efficiency as well as better fuel economy. Some technologies that have contributed to the better performance of downsized engines are boosting technologies, exhaust gas recirculation, the integration of gasoline direct injection (GDI) into engine design. Engine downsizing is, however, limited due to abnormal combustion behavior. The abnormal combustion behavior is induced by the fuel's chemical properties. Some examples of abnormal combustion behavior are engine knock and low speed pre-ignition (LSPI). Knock occurs in spark ignition engines when the fuel and air mixture in the combustion chamber ignites before the spark plug can ignite the fuel and air mixture. When the fuel and air mixture in the combustion chamber ignites before the spark plug can ignite the mixture it is called auto-ignition. Engine knock can lead to timing issues and cause damage to the engine. Low speed pre-ignition (LSPI), or super-knock, is like engine knock and has become more prevalent with downsized engines. In the past the anti-knock quality of fuels has been measured using RON and MON however due to engine downsizing it has become more difficult to predict when engine knock or LSPI will occur based on RON and MON alone. For this reason, it important to take a closer look at what the RON and MON measurements are indicating.

To understand the relationships between the chemical functional groups and RON/MON TRFs were used as surrogates to emulate a real fuel. FACE D gasoline was

the target fuel with a RON value of 94.3 and a MON value of 87. The mole fractions of toluene, n-heptane, and iso-octane were varied by 0.01 and 5,151 TRF surrogate mixtures were produced. The RON and MON values of the TRFs were determined using the quantitative structure property relationship (QSPR) regression models discussed in the next chapter. Constraints were imposed on the TRF surrogate mixtures to evaluate how effectively RON and MON could constrain the chemical structures of a gasoline surrogate. Starting with 5,151 mixtures, 358 mixtures were constrained by the RON value of the target fuel, 377 mixtures were constrained by the MON value of the target fuel, and 130 mixtures were constrained by both the RON and MON value of the target fuel. **Figure 2.3** shows the chemical functional group distributions based on mass fraction. The error bars indicate the variability of each functional group under the imposed constraints.

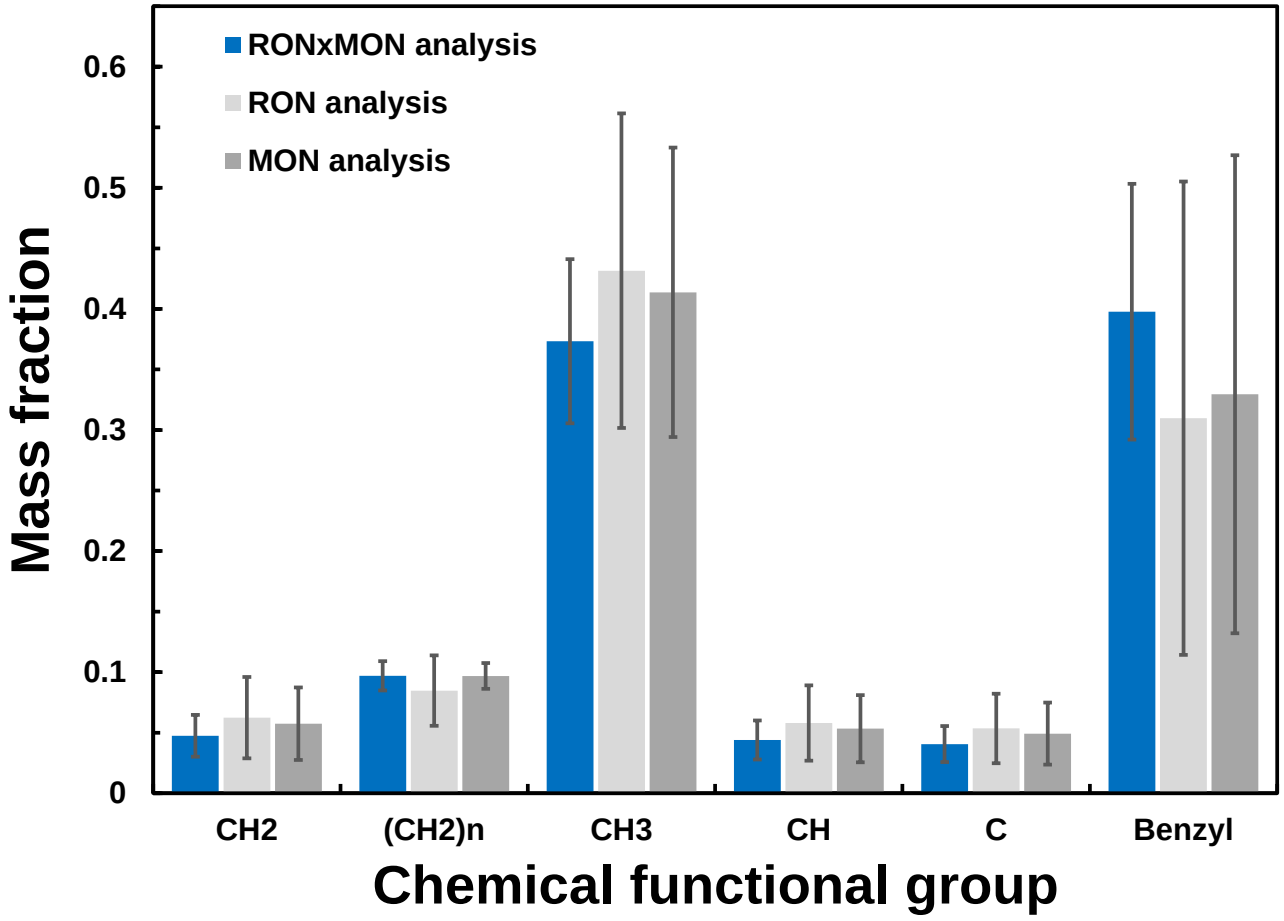

Figure 2.3. Chemical functional group distribution of TRF mixtures based on mass fraction.

Despite 139 TRF mixtures having the same RON and MON as the target fuel there were substantial variations in the chemical functional group distributions and chemical compositions of the surrogate mixtures. For this reason, two mixtures with the same RON and MON as the target fuel were further analyzed. One of the chosen TRF mixtures contained a higher concentration of aromatic content and a slightly higher concentration of the $(CH_2)_n$ functional group. The other TRF mixture contained a lower concentration of aromatic content and a slightly lower concentration of the $(CH_2)_n$ functional group. **Table 2.1** shows the mole fractions of the two TRF surrogate mixtures. **Figure 2.4** shows the chemical functional group distributions, based on mass fraction, of the two TRF mixtures.

Table 2.1. Mole fraction of two TRF surrogate mixtures.

Mole fraction	iso-octane (iC8)	n-heptane (nC7)	toluene
High aromatic content mixture	0.07	0.16	0.77
Low aromatic content mixture	0.64	0.12	0.24

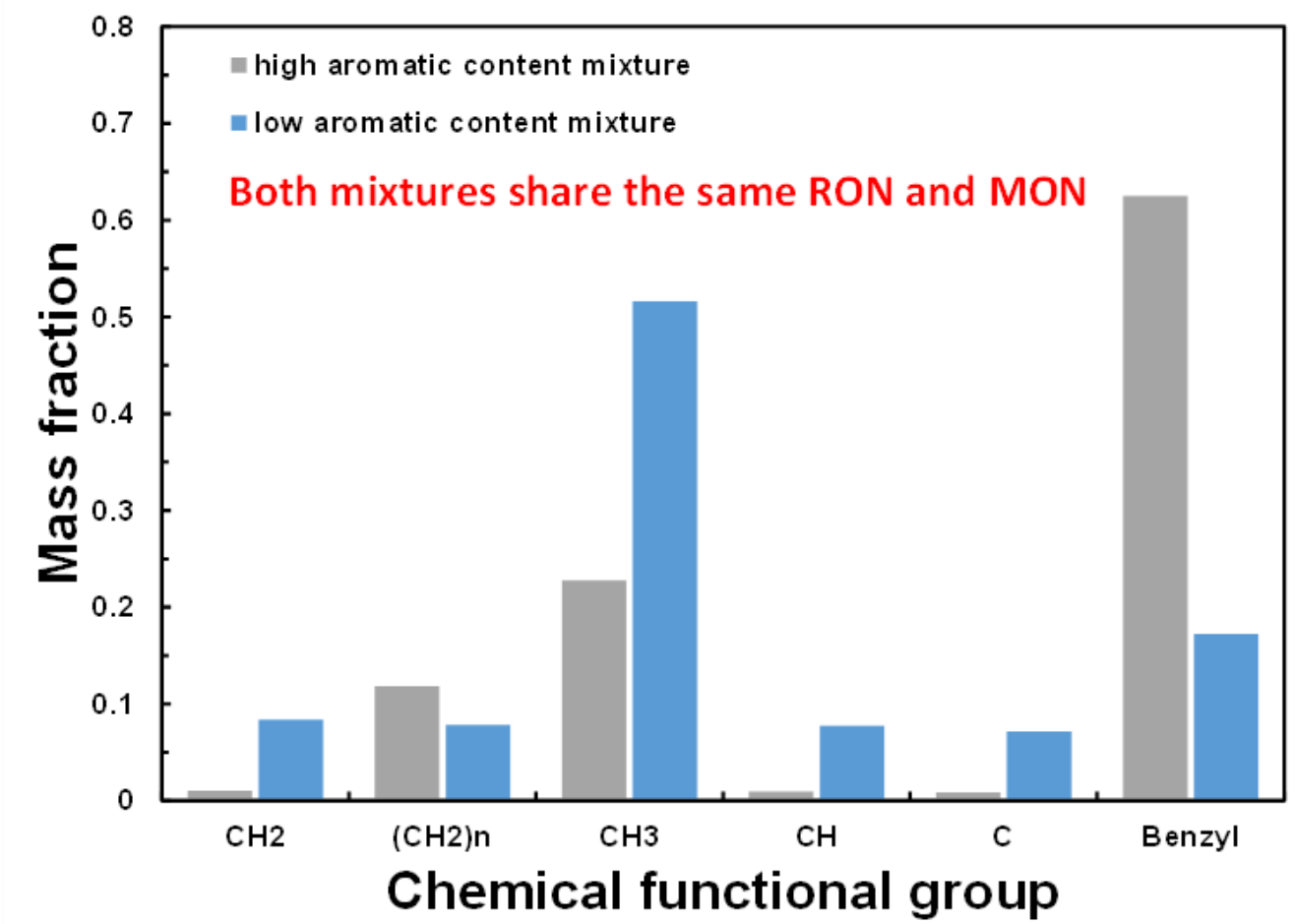

Figure 2.4. Chemical functional group distribution of two TRF mixtures.

A chemical kinetic model from Heinz Pitsch's group at Aachen was used to analyze the ignition propensity of the two surrogate mixtures [11, 12], [13]. The simulation emulates a homogeneous charged compression ignition (HCCI) process using a Chemkin tool. At an initial temperature of 450 K and an initial pressure of 0.9 atm with a compression ratio of 15 and an engine speed of 2400 rpm the ignition delay time of the low aromatic fuel was shorter. This behavior can be expected because the benzyl-type functional group, stemming from aromatics, is known to slow down overall reactivity causing a longer ignition delay time. When 100 ppm of NO was added to the system there was a shift in the ignition delay time for both fuels however for the fuel with higher aromatic content and a slightly higher concentration of the $(CH_2)_n$ functional group the shift was relatively larger. **Figure 2.5** shows the data from the simulation for the two mixtures before and after NO addition. From this analysis it was observed that RON and MON are not sufficient to predict when engine knock or LSPI will occur. The analysis also shows that aromatic content is not an appropriate measure for when engine knock or LSPI will occur, and fuel with a higher $(CH_2)_n$ content is more sensitive to ignition perturbation by either residual NO from the prior cycle left in the cylinder or NO introduced to the combustion chamber by exhaust gas recirculation.

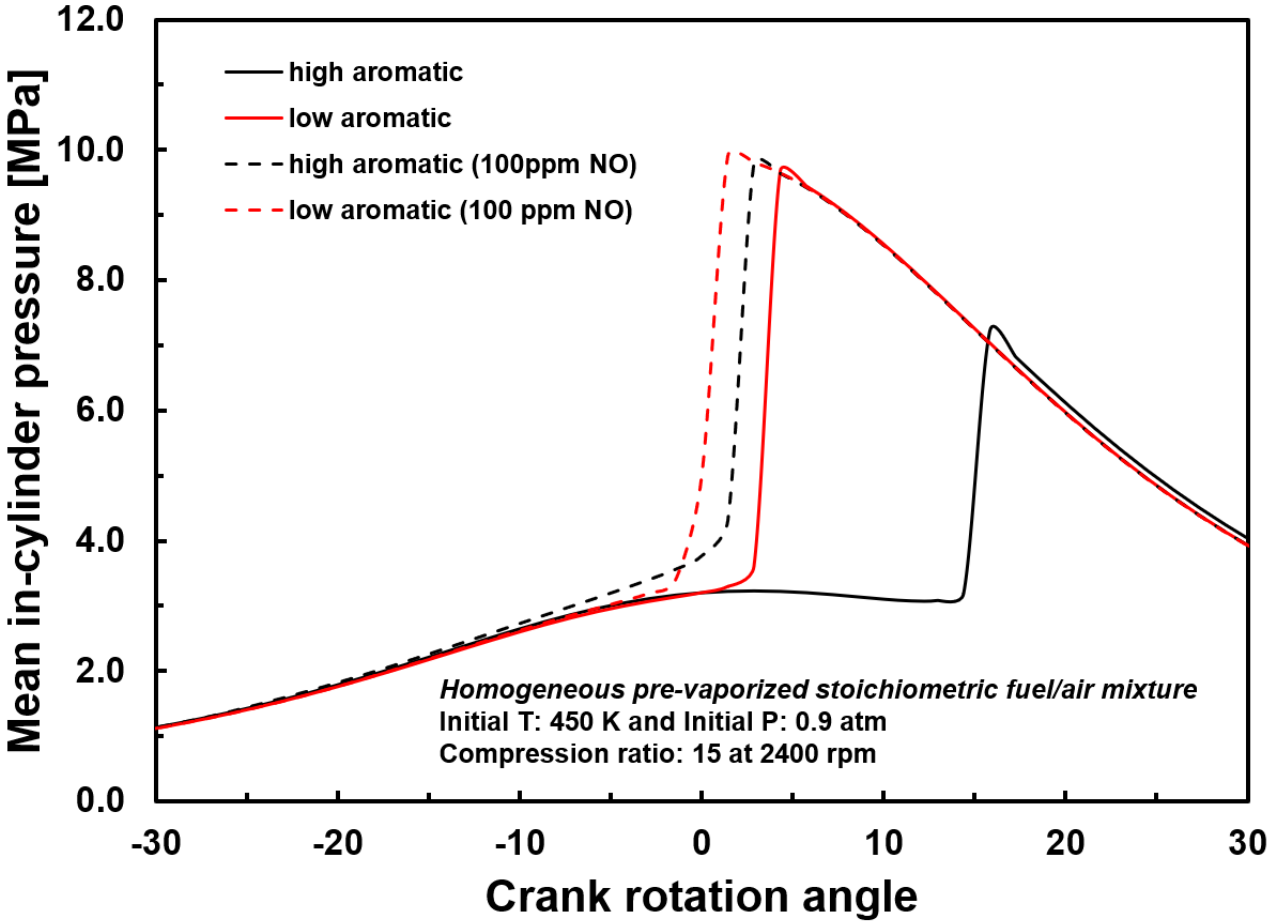

Figure 2.5. Homogeneous charge compression ignition of two TRF mixtures.

There were three main goals of the current research. The first goal was to interpret the role(s) of RON and MON through chemical functional group analysis based on databases found in the literature. RON and MON are empirically determined and used to quantify the quality of fuel, but the fundamentals of what RON and MON are physically indicating are still not well understood. The second goal was to relate RON and MON to DCN using the chemical functional group analysis. QSPR regression models were developed using the chemical functional groups. The QSPR regression models were trained using data in the literature [8] and data from the current research for RON, MON, and DCN. The QSPR regression models were then used to relate RON and MON to DCN through the chemical functional group descriptors. The third goal was to investigate the role(s) of NO addition on the ignition propensity of TRFs experimentally using DCN measurements. Residual NO can remain in the combustion chamber of an internal combustion engine after a cycle has finished or be introduced to the combustion chamber through exhaust gas recirculation. The remaining NO can influence the combustion behavior of the fuel and air mixture in the cylinder. The third goal is to observe the interactions of NO with the chemical functional groups so that the causes of engine knock and LSPI can be further understood.

CHAPTER 3

METHOD

To interpret the role(s) of RON and MON through chemical functional group analysis and to relate RON and MON to DCN through the chemical functional group descriptors it was necessary to develop QSPR regression models for RON, MON, and DCN. The QSPR regression models were based on Scheffé-simplex polynomial equations similar to the ones used in [8] however the polynomials developed in the current research were based on chemical functional group distribution rather than molar concentration of chemical components. **Equation 3.1** shows the general QSPR regression model used in the current research. In **Equation 3.1** β_0, β_i, and β_{ij} are coefficients determined through the regression analysis, x_i and x_j are the number density of the chemical functional groups, n is the number of chemical functional groups used in the regression analysis, and η is the quantity that the regression analysis is being used to model (i.e. RON, MON, or DCN). The first term in **Eq. 3.1** (β_0) is a constant used for correction, the second term in **Eq. 3.1** ($\sum_{i=1}^{n} \beta_i * x_i$) interprets the influence of each of the individual chemical functional groups on the quantity being analyzed, and the third term in **Eq. 3.1** ($\sum_{i=1}^{n-1} \sum_{j=i+1}^{n} \beta_{ij} * x_i * x_j$) interprets the influence of the interactions between the chemical functional groups on the quantity being analyzed.

$$\eta = \beta_0 + \sum_{i=1}^{n} \beta_i * x_i + \sum_{i=1}^{n-1} \sum_{j=i+1}^{n} \beta_{ij} * x_i * x_j \quad (3.1)$$

There were six chemical functional groups used in the QSPR regression model of the current work however it will be discussed later that some of the chemical functional groups had insignificant contributions to the quantities being analyzed and could be neglected. The six chemical functional groups used were the $(CH_2)_n$ functional group, the CH_3 functional group, the CH_2 functional group, the CH functional group, the C functional group, and the benzyl-type functional group. The cycloalkyl functional group, $(CH_2)_{cyclo}$, was not included in the current QSPR regression models. Further investigation of the cycloalkyl functional group is done in [14].

To investigate the role(s) of NO on the ignition propensity of TRFs using DCN measurements it was necessary to use the ignition quality tester (IQT). The IQT is a system that uses a constant volume combustion chamber to measure the ignition quality of fuels. The IQT system is composed of a base unit, a closed loop cooling system, an electrical cabinet, a computer-based system that performs data acquisition and analysis, a wheeled cabinet that holds the base unit and the cooling system, and an Uninterruptible Power Supply (UPS). The base unit includes a stainless-steel combustion chamber, a fuel injection system, and associated valves, sensors, and hardware. The IQT system uses scientific air with molar concentrations of 21% O_2 and 79% N_2. The combustion chamber maintains a pressure of 310 psi. The temperature of the combustion chamber is approximately 585^{o}C and the volume of the combustion chamber is 213 cm^3.

Before each test run the injection pump, fuel line, and injector nozzle are purged with 50 psi N_2. Once the system has been purged the next fuel to be tested is used to flush out any remaining fuel from the previous test. The injector pump is then filled with approximately 50 ml to 100 ml of the next fuel to be tested. The amount of fuel added depends on the number of runs required. The automated test procedure begins with charging the combustion chamber with the scientific air (79% N_2 and 21% O_2) to the test pressure of 310 psi. Approximately 100 mg of fuel is then injected into the combustion chamber and the time between fuel injection and a pressure rise in the combustion chamber is measured. This time interval is called the ignition delay time (IDT) and varies depending on which fuel is introduced into the IQT system. For more volatile fuels the IDT is shorter. The derived cetane number (DCN) is then calculated based on **Eq. 3.2** if the IDT is in the range of 3.1 ms to 6.5 ms and **Eq. 3.3** if the IDT is outside of the range. During a test 32 injection are performed and the average DCN of the fuel is determined as well as the standard deviation for the test.

$$DCN = 4.46 + \frac{186.6}{IDT} \tag{3.2}$$

$$DCN = 83.99 * (IDT - 1.512)^{-0.658} + 3.547 \tag{3.3}$$

To further investigate the effects of nitrogen monoxide (NO) on combustion behavior modifications were made to the IQT system. A mixing tank was added to the IQT system so that a homogeneous mixture of N_2, O_2, and NO could be prepared. The mixing tank was connected to the IQT system using various valves so that the mixture prepared in the mixing tank could replace the scientific charge air of the original IQT

system. The mixing tank was connected to the IQT system is such a way that either the original scientific air or the mixture prepared in the mixing tank could be used. This was necessary to calibrate the IQT, according to ASTM D6890 standard, as well as to verify the integrity of the mixing tank by comparing the DCN values obtained with the mixing tank to the calibrated DCN values of the original IQT system.

To perform three test runs it was necessary to fill the mixing tank to a pressure of 1500 psi. The mole fractions of the N_2, O_2, and NO in the mixing tank could be varied by changing the partial pressure of each of the components in the mixing tank. The NO used for the current research could only be purchased in diluted quantities because of the toxicity of NO. The highest NO concentration that could be purchased was diluted with nitrogen with molar concentrations of 5% for NO and 95% for N_2. The NO/N_2 tank was connected to the mixing tank along with a tank containing only oxygen, O_2, and a tank containing only nitrogen, N_2. The amount of N_2, O_2, and NO/N_2 were varied so that the molar ratio of N_2 to O_2 could be maintained at approximately 3.76 while the molar concentration of NO was controlled. The mixing tank was also connected to a vacuum pump so that the mixing tank could be completely emptied before preparing a new mixture. The partial pressures necessary for N_2, O_2, and the NO/N_2 mixture were calculated using **Eqs. 3.4-3.6**. In **Eqs. 3.4-3.6** NO_{ppm} is the parts per million of nitrogen monoxide, P_{NO/N_2} is the partial pressure of the NO/N_2 mixture, P_{O_2} is the partial pressure of O_2, P_{N_2} is the partial pressure of the N_2 from the N_2 tank only, and P_t is the total pressure in the mixing tank (1500 psi for three runs). Each of the partial pressure equations are dependent on the partial pressure of nitrogen monoxide that is chosen to be investigated.

$$P_{NO/N_2} = P_t * \frac{NO_{ppm} + \left(\frac{1 - 0.05}{0.05}\right) * NO_{ppm}}{10^6} \quad (3.4)$$

$$P_{O_2} = P_t * \frac{\left(10^6 - NO_{ppm}\right) * 0.21}{10^6} \quad (3.5)$$

$$P_{N_2} = P_t - P_{NO/N_2} - P_{O_2} \quad (3.6)$$

To verify that the mixing tank could be used to obtain accurate data the DCN of n-heptane was measured using the mixing tank and compared to the calibrated original IQT system. The mixing tank was filled with 79% N_2 and 21% O_2 and 0 ppm NO to match the scientific air of the original IQT system. The comparison of the DCN measurements using the original IQT system and the mixing tank can be seen in **Table 3.1**. **Table 3.1** shows that the DCN of n-heptane measured using the mixing tank agrees well with the DCN measured using the original IQT system. The average DCN of the original IQT system was 53.87 with a standard deviation of 0.245 and the average DCN of the modified IQT system was 53.87 with a standard deviation of 0.2059. The agreement between the two systems verified that the mixing tank could be used to measure the DCN of n-heptane and demonstrated that the mixing tank could also be used to measure the DCN with controlled NO molar concentrations.

Table 3.1. DCN comparison between the mixing tank and the original IQT system.

Method	Run #	Fuel ID	Ignition Delay	Std Dev ID	DCN	Std Dev DCN
Original IQT System	1	heptane	3.803	0.060	53.53	0.78
	2	heptane	3.778	0.067	53.85	0.87
	3	heptane	3.774	0.073	53.90	0.96
	4	heptane	3.778	0.075	53.85	1.00
	5	heptane	3.750	0.070	54.22	0.94
Mixing Tank Test # 1	1	heptane N2/O2 mix	3.728	0.080	54.51	1.09
	2	heptane N2/O2 mix	3.749	0.071	54.23	0.94
	3	heptane N2/O2 mix	3.805	0.049	53.50	0.64
Mixing Tank Test # 2	1	heptane N2/O2 mix	3.810	0.085	53.44	1.10
	2	heptane N2/O2 mix	3.773	0.077	53.92	1.02
	3	heptane N2/O2 mix	3.794	0.052	53.64	0.67

The chemical functional group distribution for TRF mixtures can easily be determined because the molecular distribution of the TRF mixtures is known. For real fuels composed of many molecules it is more difficult to determine the chemical functional group distribution. NMR spectroscopy can be used to determine the chemical functional group distribution of real fuels. For the current research NMR spectroscopy was done for ^{1}H and ^{13}C spectra. The NMR machine used was the Bruker Avance III 400. Chromium (III) acetylacetonate ($Cr(C_5H_7O_2)_3$) was added to the NMR samples as a relaxing agent so that the relaxation delay time could be reduced. The relaxation delay time for the ^{1}H spectra was 30 seconds. The relaxation delay time for the ^{13}C spectra was 40 seconds. The solvent used for the calibration of the NMR spectroscopy was deuterated Chloroform, also known as Chloroform-D or $CDCl_3$ and the Chromium (III) acetylacetonate was added to the $CDCl_3$ until a molarity of 0.05 for Chromium (III) acetylacetonate was achieved. For the ^{1}H NMR spectra the chemical shift for $CDCl_3$ is 7.26 ppm and for the ^{13}C NMR spectra the chemical shift for $CDCl_3$ is 77.02 ppm. NMR spectroscopy was used in the current research to determine the chemical functional group

distribution of ethanol free gasoline with an AKI of 89. The chemical functional group distribution was then used with the developed QSPR regression models to predict the RON, MON, and DCN of the ethanol free gasoline as well as five distillation cuts of the ethanol free gasoline.

CHAPTER 4

RESULTS

Using the chemical functional group distribution of toluene reference fuels and the Scheffé-simplex polynomial QSPR regression models were developed for RON, MON, and DCN. **Figure 4.1** shows the relationship between the measured RON [8] and the predicted RON using the QSPR regression model developed in the current work. It is shown in **Fig. 4.1** that there is nearly a one-to-one relationship between the measured RON values and the predicted RON values from the QSPR regression model. **Figure 4.2** shows the relationship between the measured MON [8] and the predicted MON values based on the QSPR regression model developed in this study. It is shown in **Fig. 4.2** that the QSPR regression model developed in the current work based on the chemical functional group descriptors has nearly a one-to-one relationship with the measured values for MON [8]. The relative significance of the regression coefficients in the QSPR regression models was determined based on a sensitivity analysis. To achieve reasonable prediction fidelity for RON and MON only the coefficients for the $(CH_2)_n$, CH_3, and benzyl-type groups were necessary. There was no need to consider the coefficients for the interaction terms because their contributions were insignificant.

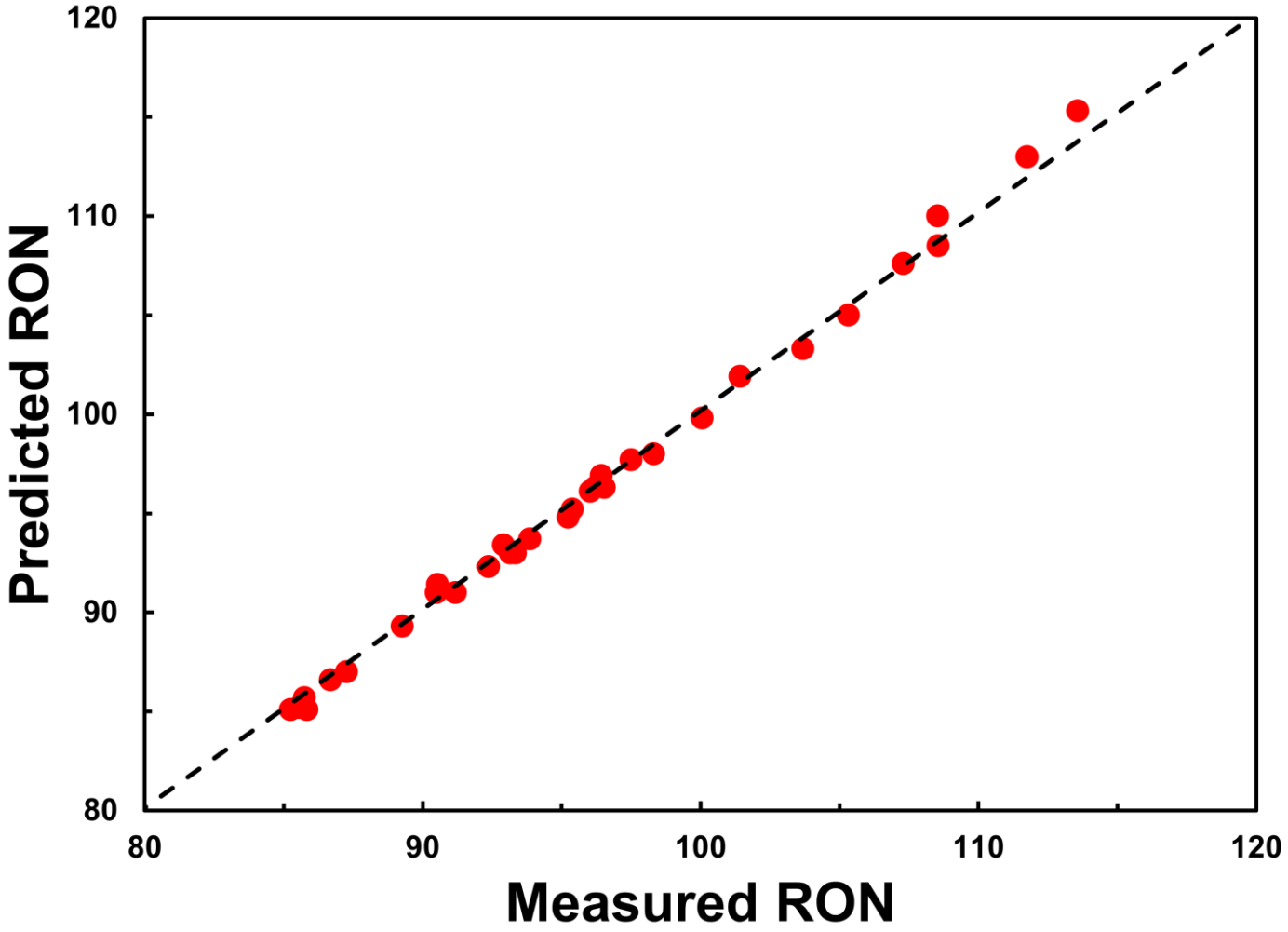

Figure 4.1. Comparison between measured RON values and predicted RON values.

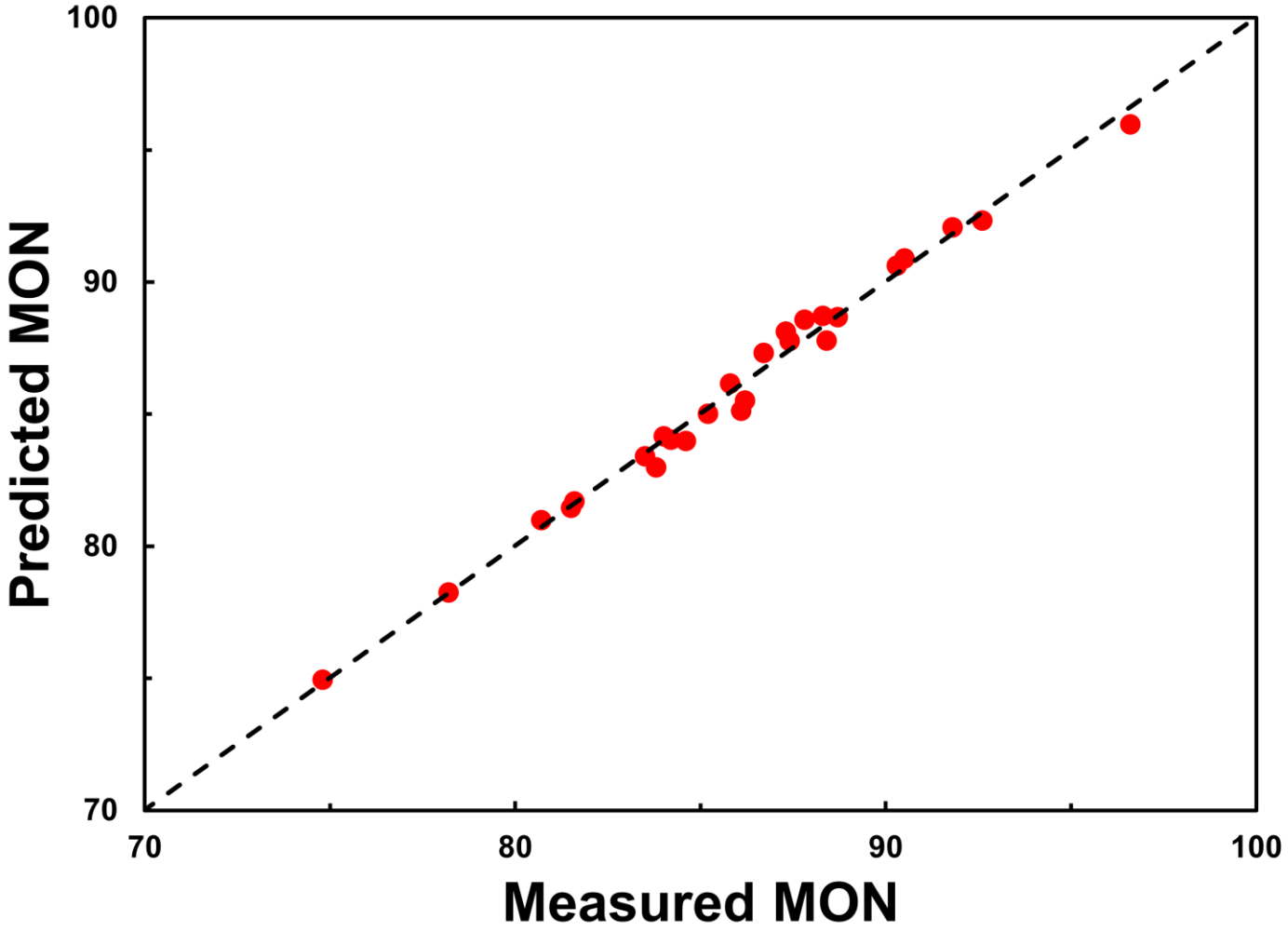

Figure 4.2. Comparison between measured MON values and predicted MON values.

The DCN values of the TRF mixtures were measured using the IQT and the measured values were used to develop a QSPR regression model for DCN based on the chemical functional group descriptors. **Figure 4.3** shows the relationship between the measured DCN values and the DCN values predicted by the QSPR regression model. The QSPR regression model developed based on the chemical functional group descriptors for DCN has a nearly one-to-one relationship with the measured DCN values. To achieve reasonable prediction fidelity for DCN the coefficients for the $(CH_2)_n$, CH_3, and benzyl-type groups were significant as well as the coefficients for the interaction terms between the $(CH_2)_n$ and CH_3 functional groups and the $(CH_2)_n$ and benzyl-type functional groups.

Once the QSPR regression models for RON, MON, and DCN were developed and a strong correlation was found between their measured values and their predicted values it was concluded that the RON, MON, and DCN could be accurately predicted using the QSPR regression models. The relationship between DCN and RON as well as the relationship between DCN and MON were then analyzed. **Figure 4.4** shows the relationship between DCN and RON. As expected, when the DCN of the TRF mixtures increased the RON decreased. A similar relationship is shown in **Fig. 4.5** between DCN and MON.

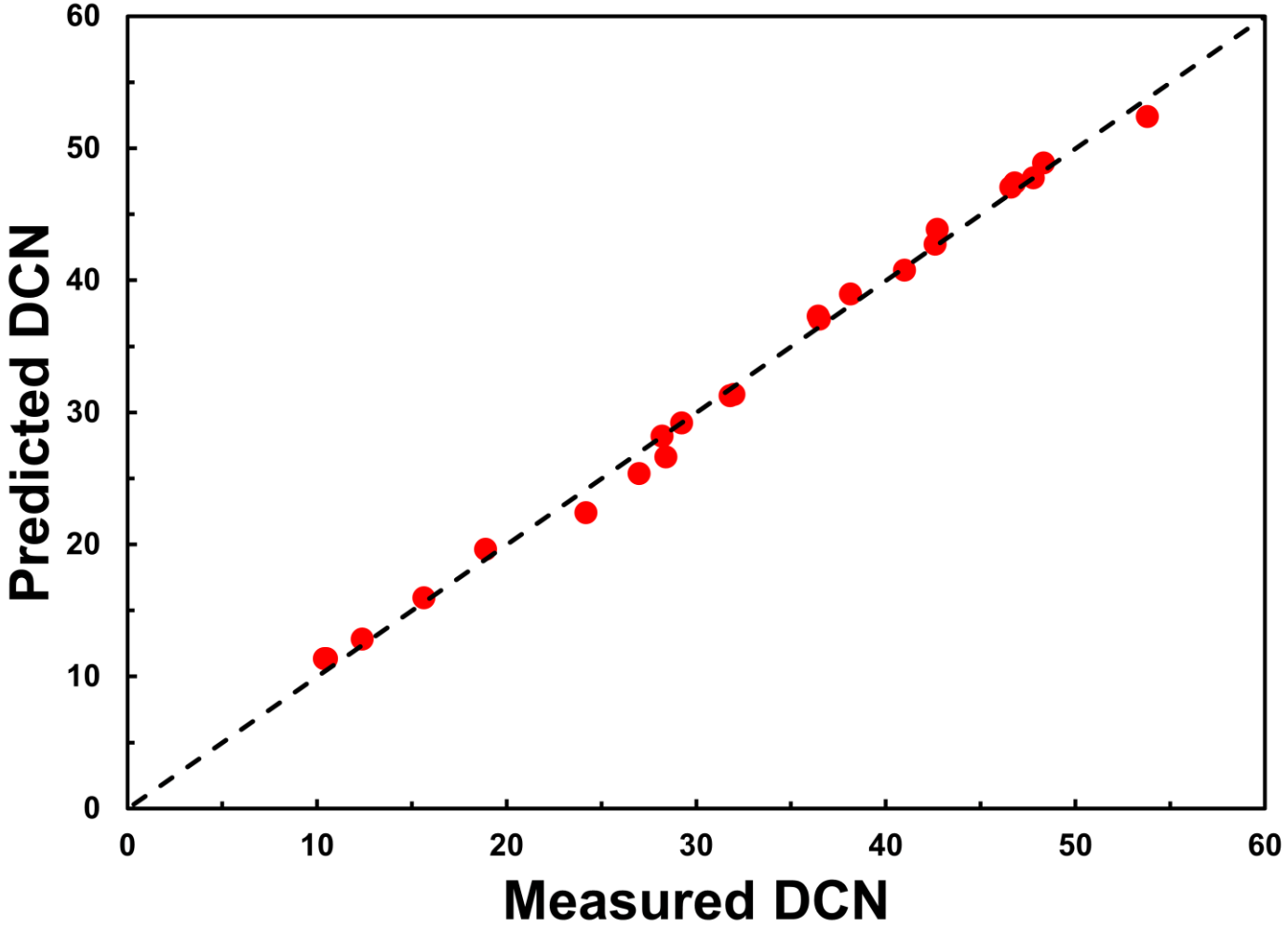

Figure 4.3. Comparison between measured DCN values and predicted DCN values.

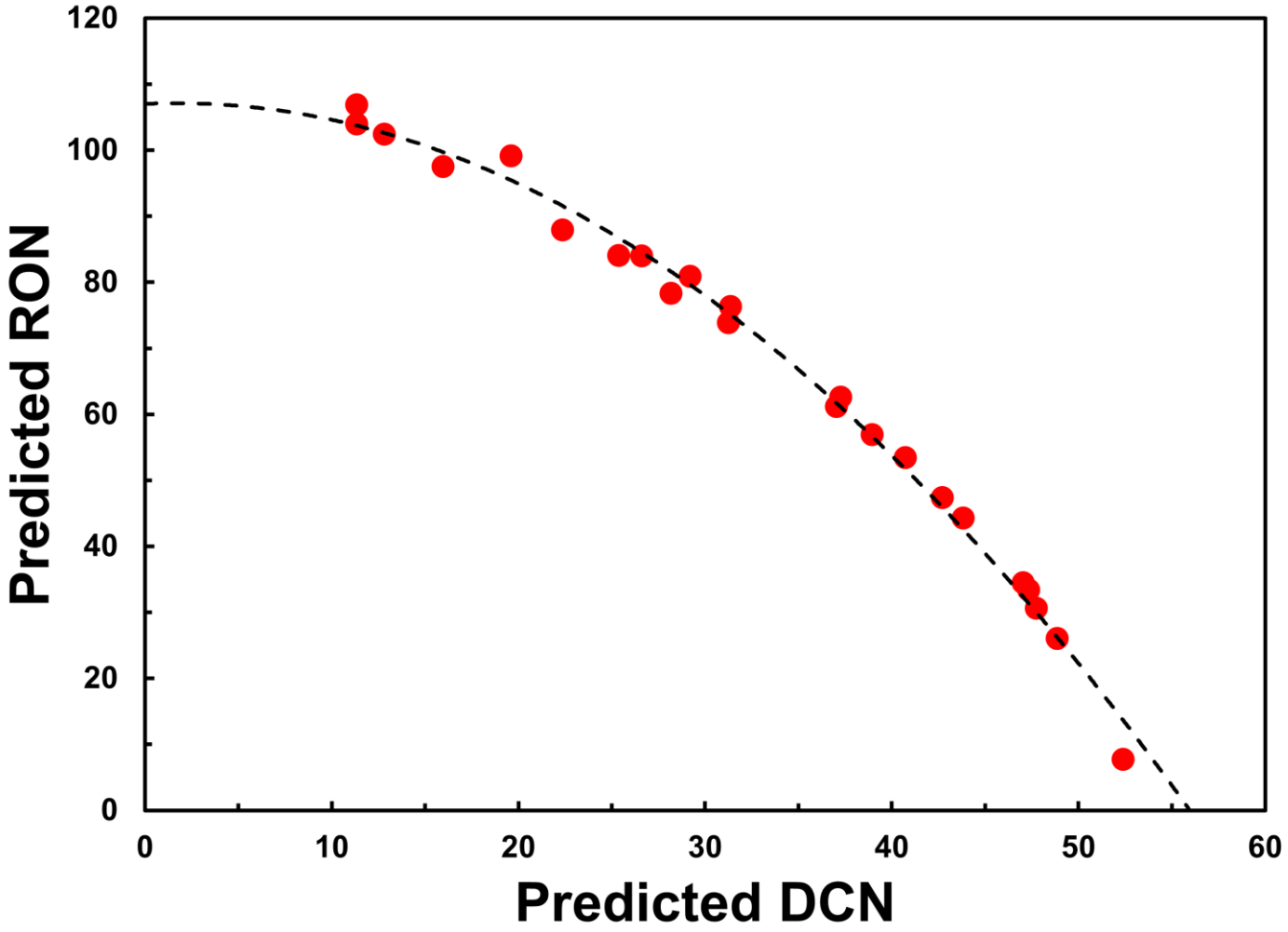

Figure 4.4. Comparison between predicted DCN values and predicted RON values.

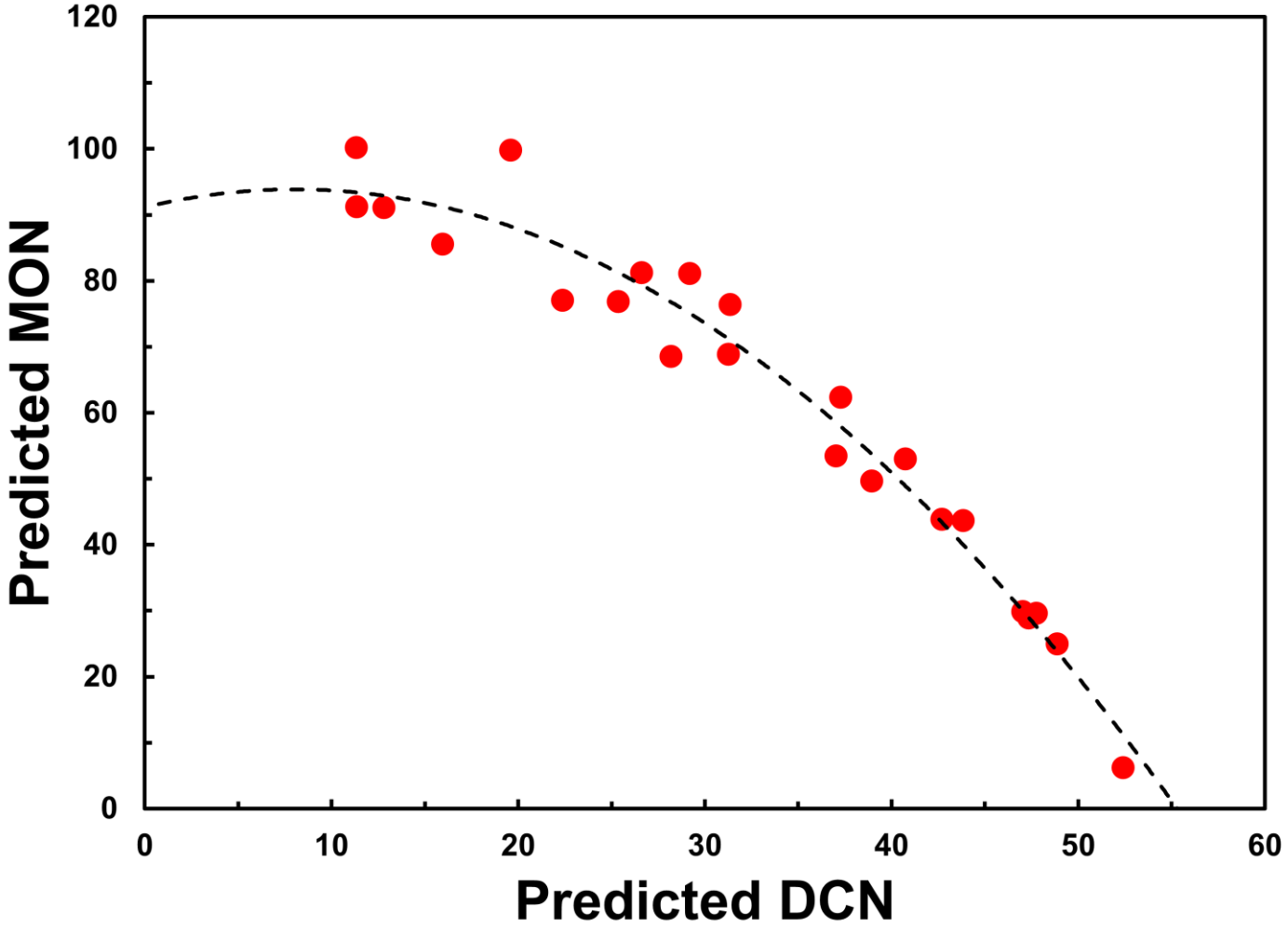

Figure 4.5. Comparison between predicted DCN values and predicted MON values.

The effects that NO has on the ignition propensity of TRFs were investigated so that the contribution of NO chemistry to engine knock and LSPI in downsized engines could be better understood. NO gas can be left in the cylinder of an internal combustion engine from remaining exhaust gases in the cylinder from the previous combustion cycle or from exhaust gas recirculation. To begin investigating the role(s) of NO on ignition propensity the effects of NO on the ignition propensity of n-heptane were first analyzed. The mole fraction of NO added to the charge air of the IQT system was controlled by changing the partial pressure of the NO/N_2 tank. The mole fraction of NO in the charge air was increased and the DCN of n-heptane was measured. The results are shown in **Fig. 4.6**. As the mole fraction of NO is increased from 0 ppm to 300 ppm there is a monotonic increase in the DCN of n-heptane. When the NO mole fraction was increased further a decrease in the DCN of n-heptane was observed until a mole fraction of 1000 ppm NO was reached.

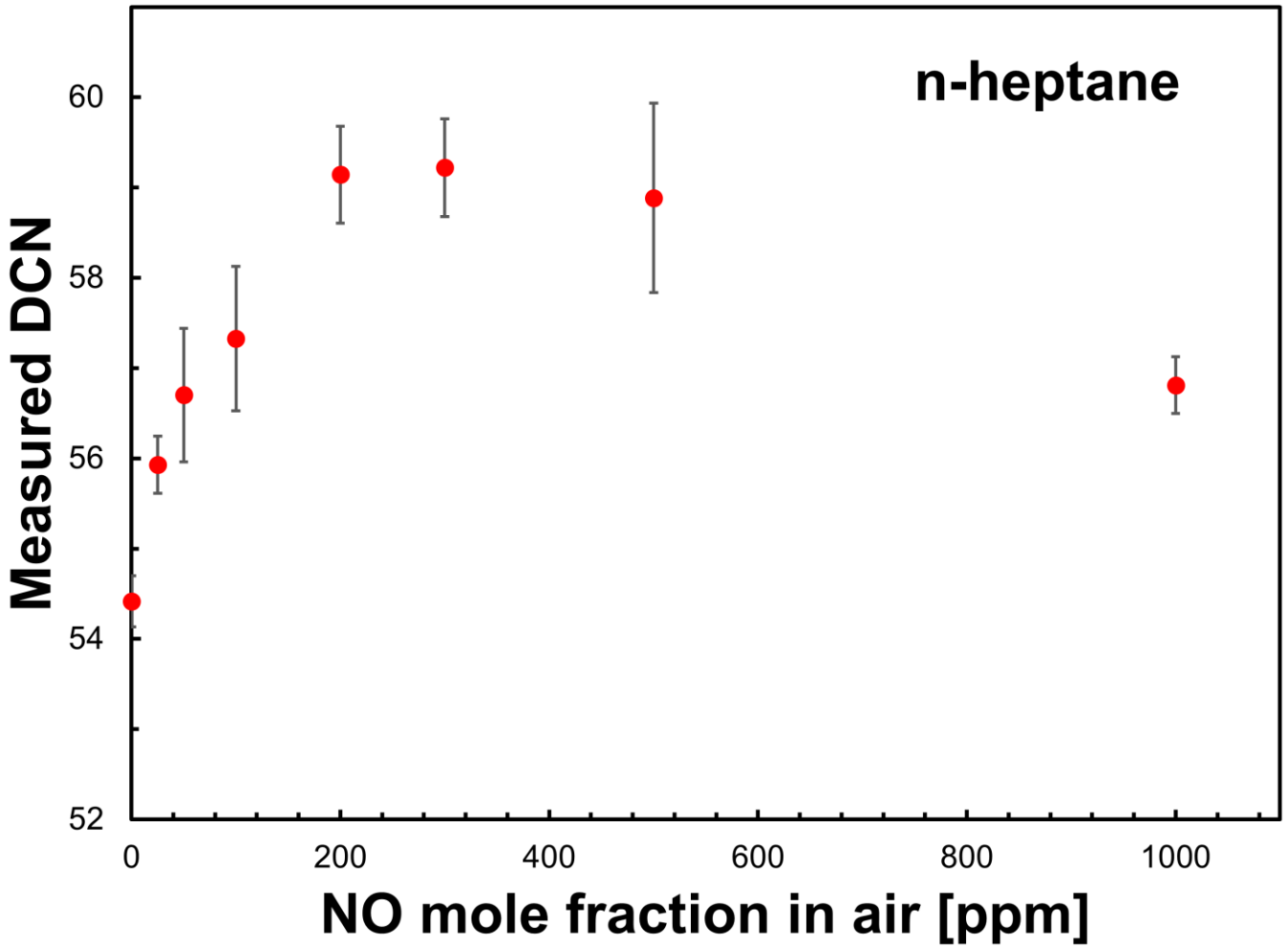

Figure 4.6. DCN of n-heptane as a function of NO mole fraction in air.

To investigate the role(s) of NO on the TRF mixtures the mole fraction of NO in the charge air was maintained at 200 ppm and the DCN of 20 TRF mixtures were measured. The mole fraction of the NO in the charge air of the IQT was chosen to be 200 ppm because this mole fraction seemed to have the largest effect on the DCN of n-heptane in the previous experiment. The mole fraction of the TRF mixtures as well as their DCN measurements before and after 200 ppm NO was added to the charge air are shown in **Table 4.1**. It was found that the change in DCN values before and after 200 ppm NO was added to the charge air is directly related to the number density of the $(CH_2)_n$ functional group. This relationship is shown in **Fig. 4.7**. It should be noted that the TRF mixture with no n-heptane (mixture # 19), and therefore no molecules containing the $(CH_2)_n$ functional group, has nearly no change in the DCN when 200 ppm NO gas was added to the charge air of the IQT system. It can be concluded that the NO added to the charge air of the IQT system has major interactions with the $(CH_2)_n$ functional group causing an increase in the ignition propensity of the TRF mixtures.

Table 4.1. Mole fractions of TRF mixtures and DCN measurements with and without 200 ppm NO addition.

TRF Mixture #	Mole Fraction			DCN	DCN with NO
	nC7H16	iC8H18	C7H8		
1	1.000	0.000	0.000	53.80	59.04
2	0.800	0.200	0.000	48.32	52.83
3	0.750	0.250	0.000	47.80	51.83
4	0.760	0.000	0.240	46.80	50.75
5	0.750	0.000	0.250	46.60	50.24
6	0.600	0.400	0.000	42.73	46.80
7	0.600	0.200	0.200	42.60	45.03
8	0.500	0.500	0.000	41.00	44.03
9	0.540	0.000	0.460	38.14	41.22
10	0.500	0.000	0.500	36.50	39.39
11	0.400	0.600	0.000	36.45	40.56
12	0.250	0.750	0.000	32.00	34.46
13	0.333	0.333	0.333	31.80	34.78
14	0.200	0.800	0.000	29.23	32.02
15	0.200	0.600	0.200	28.40	29.89
16	0.340	0.000	0.660	28.21	30.91
17	0.250	0.250	0.500	27.00	28.54
18	0.250	0.000	0.750	24.20	25.41
19	0.000	1.000	0.000	18.90	18.99
20	0.160	0.000	0.840	15.65	17.49

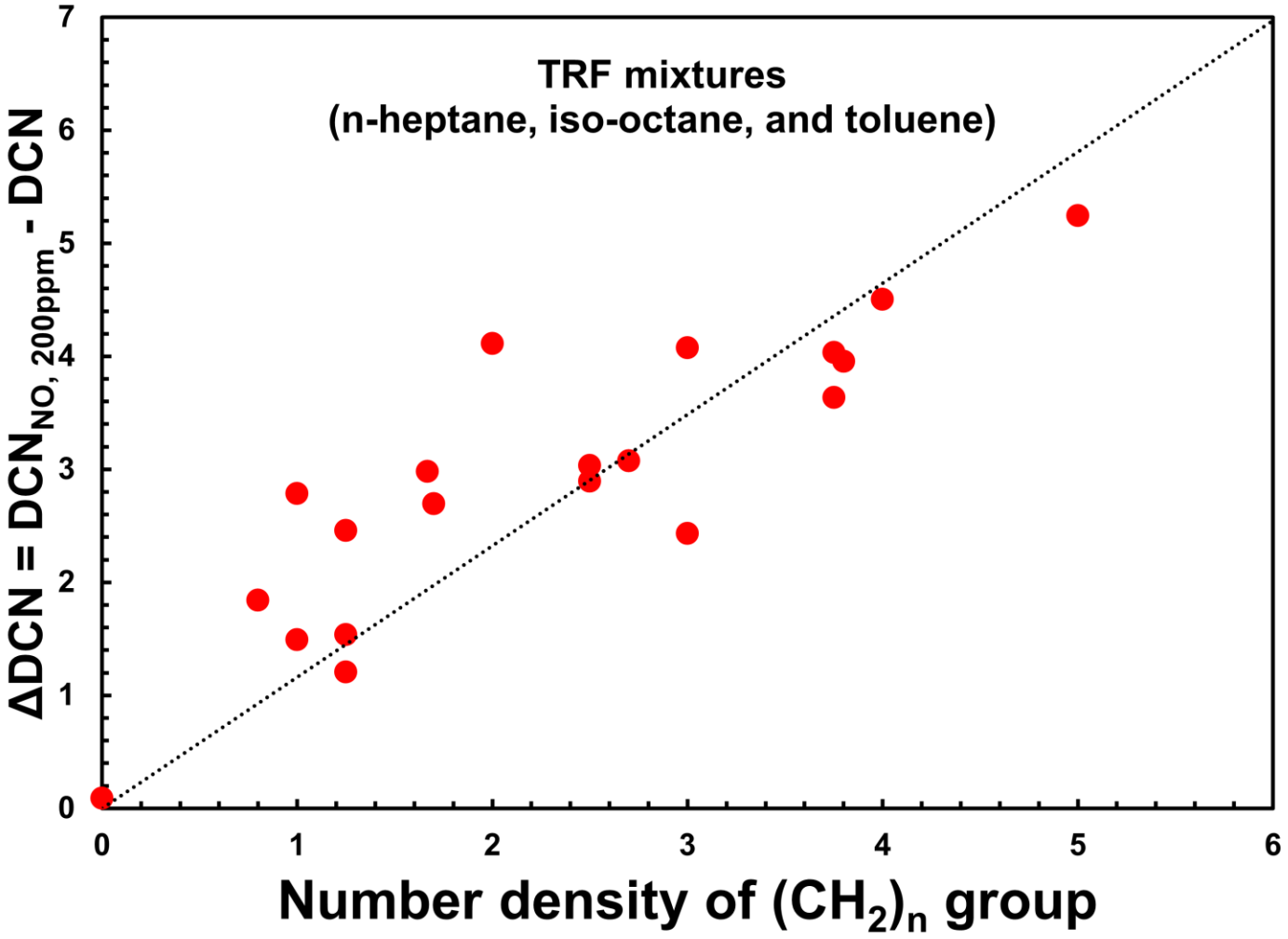

Figure 4.7. Relationship between the number density of the $(CH_2)_n$ functional group and the change in DCN after adding 200 ppm NO.

After analyzing the effects of NO on the DCN of the TRF mixtures a gasoline fuel was investigated. The gasoline chosen was an ethanol free gasoline with an AKI of 89. The ^{1}H NMR spectra as well as the ^{13}C NMR spectra were taken for the ethanol free gasoline. Five distillation cuts were taken from the ethanol free gasoline and the ^{1}H NMR spectra as well as the ^{13}C NMR spectra were taken for the five distillation cuts. The ^{1}H NMR spectra for the ethanol free gasoline with an AKI of 89 is shown in **Fig. 4.8** and the ^{13}C NMR spectra for the same ethanol free gasoline is shown in **Fig. 4.9**. The chemical functional group distribution of the ethanol free gasoline is shown in **Fig. 4.10** and was determined based on the chemical shifts of the NMR spectra.

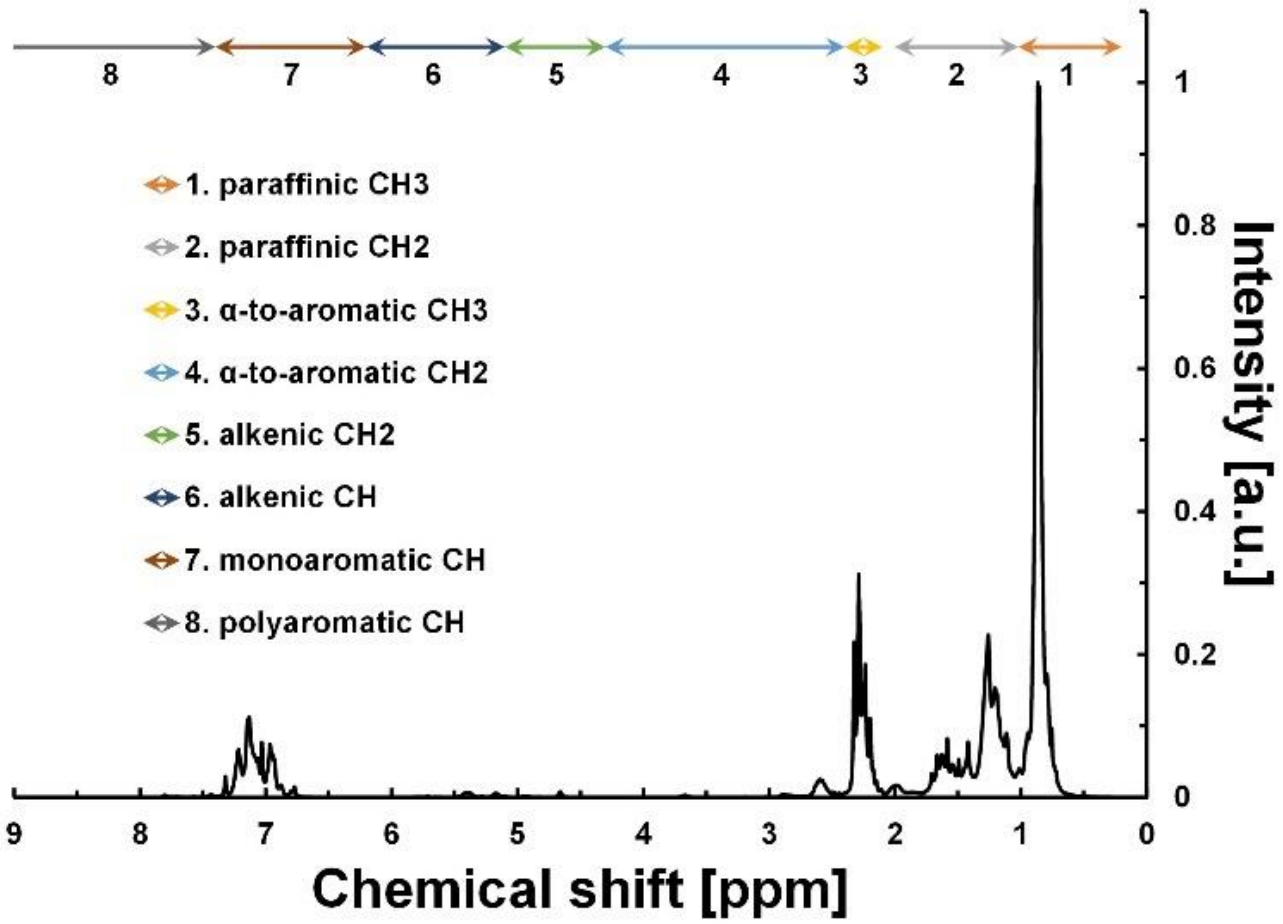

Figure 4.8. ^{1}H NMR spectra for ethanol free gasoline.

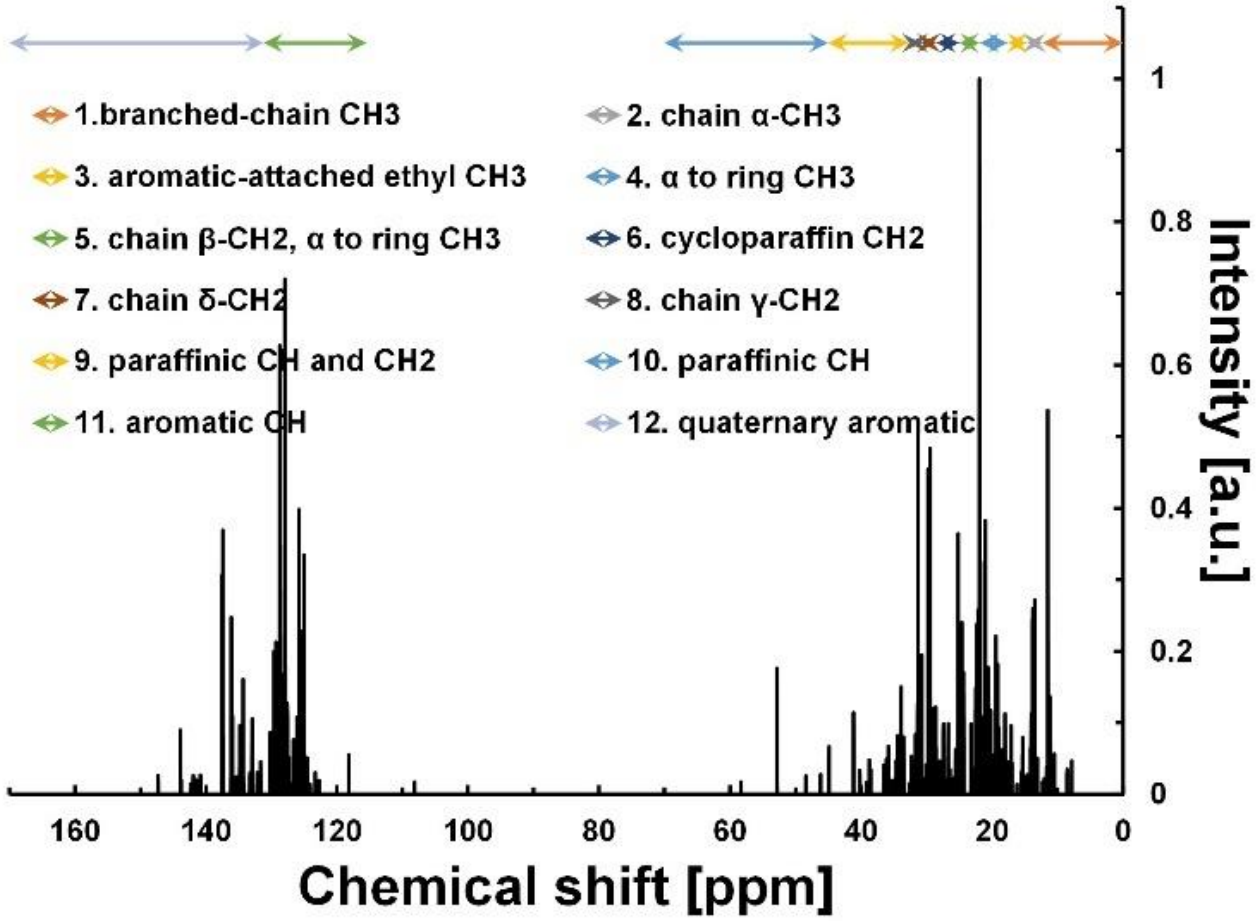

Figure 4.9. ^{13}C NMR spectra for ethanol free gasoline.

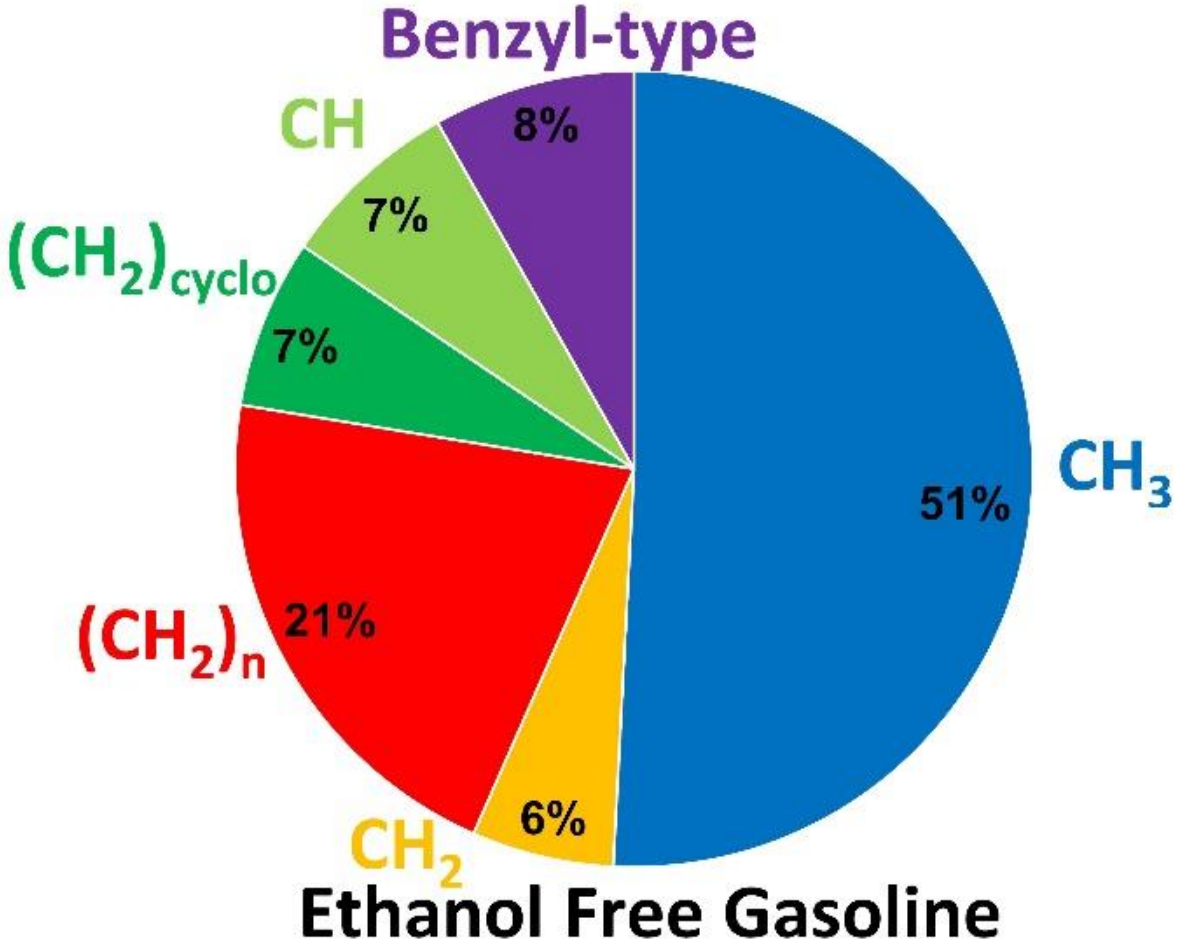

Figure 4.10. Chemical functional group distribution of ethanol free gasoline (AKI 89).

Figure 4.11 shows the mole fraction of the CH_3, $(CH_2)_n$, and benzyl-type functional groups in each of the five distillation cuts. It is shown in **Fig 4.11** that the mole fraction of the CH_3 functional group does not change very much throughout the distillation process and stays close to the CH_3 mole fraction of the neat fuel. The mole fraction of the $(CH_2)_n$ functional group decreases from the lighter end of the distillation cuts to the heavier end of the distillation cuts. The mole fraction of the benzyl-type functional group increases from the lighter end of the distillation cuts to the heavier end of the distillation cuts. Based on the previous understanding of the roles played by the $(CH_2)_n$ functional group and the benzyl-type functional group it was expected that the DCN should decrease from the lighter end of the distillation cuts to the heavier end of the distillation cuts and the RON, and MON, should increase from the lighter end of the distillation cuts to the heavier end of the distillation cuts.

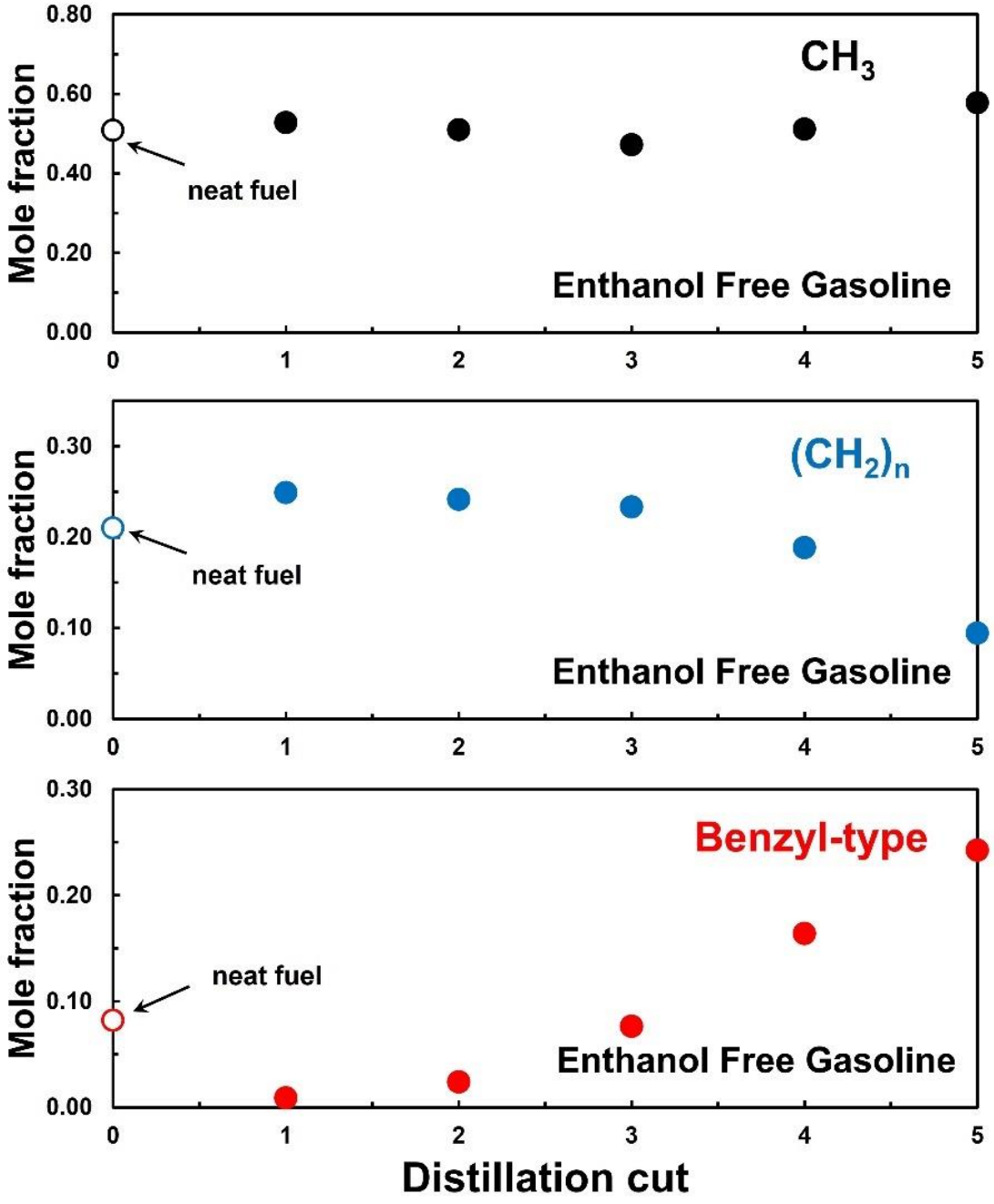

Figure 4.11. Mole fraction of CH_3, $(CH_2)_n$, and benzyl-type functional groups of five distillation.

Figure 4.12 shows the predicted RON and DCN values of the distillation cuts using the QSPR regression models developed previously. As expected, the predicted RON value increases from the lighter end of the distillation cuts to the heavier end of the distillation cuts and the predicted DCN value decreases from the lighter end of the distillation cuts to the heavier end of the distillation cuts. The RON of the distillation cuts was predicted using the QSPR regression model developed in the current study but was not measured because there is not a CFR engine in the lab. The correlation between the measured RON [8] and the predicted RON using the QSPR regression model validates the use of the QSPR regression model to predict RON. The trend of the predicted RON values for the ethanol free gasoline distillation cuts will agree with the trend of the measured RON values. The DCN of the ethanol free gasoline was predicted using the QSPR regression model developed in the current study but was not measured because the low DCN of the ethanol free gasoline could cause damage to the IQT system. The correlation between the measured DCN values and the predicted DCN values using the QSPR regression model validates the use of the QSPR regression model to predict DCN. The trend of the predicted DCN values for the ethanol free gasoline distillation cuts will agree with the trend of the measured DCN values.

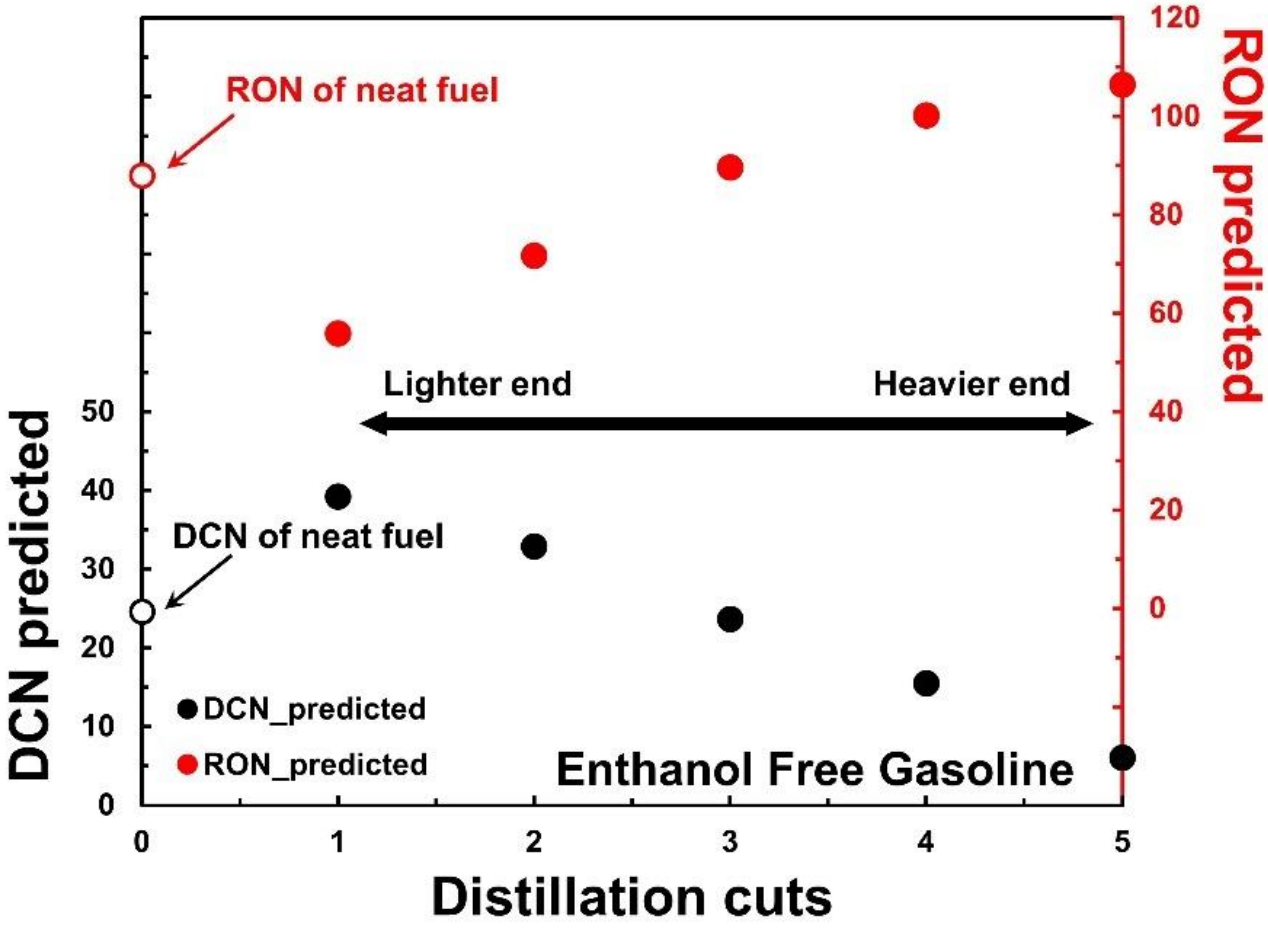

Figure 4.12. Predicted DCN and predicted RON of five distillation cuts.

By studying the interactions between NO and the chemical functional groups it was determined that the interactions between NO and the $(CH_2)_n$ functional group increase the ignition propensity of fuels. Using NMR spectroscopy, the chemical functional group distributions of an ethanol free gasoline and five distillation cuts of the ethanol free gasoline were determined. By analyzing the chemical functional group distributions of the distillation cuts of the ethanol free gasoline it was found that the $(CH_2)_n$ functional group concentration decreased from the lighter end of the distillation cuts to the heavier end of the distillation cuts. It was also found that the benzyl-type functional group concentration increased from the lighter end of the distillation cuts to the heavier end of the distillation cuts. As predicted, from the understanding of the chemical functional groups and their behaviors, the DCN decreased from the lighter end of the distillation cuts to the heavier end of the distillation cuts whereas the RON increased from the lighter end of the distillation cuts to the heavier end of the distillation cuts.

From this understanding of the interactions between NO and the $(CH_2)_n$ functional group it can be assumed that the engine knock and LSPI occurring in smaller downsized engines is due to the interactions between NO in the cylinder, either from the previous cycle or from exhaust gas recirculation, and the $(CH_2)_n$ functional group in the lighter end of gasoline. When the lighter end of the gasoline evaporates it is more likely to ignite if NO is present in the cylinder. The interactions between the vaporized portion of the gasoline and the NO present in the cylinder may cause ignition to occur before the prescribed time causing knock or LSPI.

CHAPTER 5

CONCLUSION

Energy is one of the most in demand products in the world and as more countries in the world develop the demand for energy will continue to increase. Currently most of the energy produced in the world is produced by burning fossil fuels such as coal, petroleum, and natural gas. The harmful environmental effects of burning fossil fuels have led to a higher demand for renewable energy sources however the amount of energy produced by renewable energy sources cannot currently meet energy demands. To meet the energy demands of the future it will still be necessary to burn fossil fuels, but the goal in the meantime is to make the burning of fossil fuels as efficient as possible and to minimize the harmful emissions related to burning fossil fuels.

Internal combustion engines, such as spark ignition engines and compression ignition engines, are used to produce energy by burning petroleum derived fuels. Diesel fuel is usually burned in compression ignition engines while gasoline is usually burned in spark ignition engines. The quality of fuels burned in internal combustion engines is quantified using standardized methods and standardized quantities. Two of the main quantities used to measure the quality of gasoline fuel are the Research octane number (RON) and the Motor octane number (MON). A third quantity used to measure the quality of gasoline fuel is the anti-knock index (AKI). The AKI is the averaged value of the RON and MON of a given fuel. The RON, MON, and AKI are all quantities used to

determine how well a spark ignition engine resist engine knock. Knock occurs when the fuel and air mixture in the combustion chamber of a spark ignition engine ignites before the spark igniter has the chance to ignite the fuel and air mixture. Engine knock can cause timing issues and cause permanent engine damage if the engine knock is extreme. The quality of diesel fuels is usually quantified by the cetane number (CN) or the derived cetane number (DCN). Both the CN and the DCN measure the ignition quality of the fuel being tested. For compression ignition engines there is no spark to initiate the combustion process. The fuel and air mixture in a compression ignition engine is ignited by the high temperature and pressure conditions in the combustion chamber. If a given fuel has a high ignition propensity, then the fuel will have a high CN and a high DCN.

Many advancements have been made to the design of internal combustion engines. Boosting technologies as well as the emergence of exhaust gas recirculation have led to better engine performance as well as reduced emissions. Exhaust gas recirculation also contributes to better thermal efficiency. However, despite the advancements made in the design of internal combustion engines, they are still known to emit unburned hydrocarbons (UHC), oxides of nitrogen (NO_x), oxides of sulfur (SO_x), carbon monoxide (CO), and carbon dioxide (CO_2). When exhaust gases remain in the cylinder of an internal combustion engine or are recirculated into the fuel and air mixture of the cylinder the products of the combustion process can influence the chemical reactions of the next combustion cycle.

Real petroleum derived fuels are composed of hundreds and sometimes thousands of chemical components. When there are many chemical components, it is difficult to predict the chemical pathways that each chemical component will take in the combustion

process. It has been found that the overall combustion behavior can be predicted based on the distribution of chemical functional groups [14]. Chemical functional groups are fragments of molecules that behave in similar ways throughout the combustion process regardless of the molecule they are attached to. The chemical functional groups used in the current research were the linearly bonded methylene group ($(CH_2)_n$ where "n" indicates the resulting carbon chain length), the isolated methylene group (CH_2), the methyl group (CH_3), the benzyl-type group, the CH group, and the C group. The chemical functional group distribution of known chemical mixtures can be easily determined. Toluene reference fuels (TRFs, mixtures of n-heptane, iso-octane, and toluene) were used as surrogates for petroleum derived fuels to construct Quantitative structure property relationship (QSPR) regression models for RON, MON, and DCN based on the chemical functional group distribution of the TRFs. Once the QSPR regression models were developed they could be used to determine the RON, MON, and DCN of any fuel if the chemical functional group distribution was known.

The effects of NO on the ignition propensity of TRF mixtures were also investigated. First the effects of NO on the ignition propensity of n-heptane were examined using an IQT. The mole fraction of NO in the charge air of the IQT system was increased and the change in the DCN of n-heptane was measured. It was found that there was a monotonic increase in the DCN of n-heptane from 0 ppm NO to 300 ppm NO. When the NO concentration in the charge air was increased beyond 300 ppm there was a decrease in the DCN until an NO concentration of 1000 ppm. The effects of NO on TRFs were then investigated and the concentration of NO in the charge air was maintained at 200 ppm. This concentration was chosen because this concentration seemed to have the

largest effect on the ignition propensity of n-heptane in the previous experiment. It was found that the increase in the ignition propensity of the TRFs with 200 ppm NO added to the charge air was directly related to the mole fraction of the $(CH_2)_n$ functional group.

NMR spectroscopy was then used to determine the chemical functional group distribution of a gasoline fuel. The fuel used was an ethanol free gasoline with an AKI of 89. The NMR spectroscopy was done for the neat fuel and for five distillation cuts of the ethanol free gasoline. It was found that the mole fraction of the $(CH_2)_n$ functional group decreased from the lighter end of the distillation cuts to the heavier end of the distillation cuts. It was also found that the mole fraction of the benzyl-type functional group increased from the lighter end of the distillation cuts to the heavier end of the distillation cuts. The DCN and RON of the neat ethanol free gasoline and each of the five distillation cuts were then predicted based on the QSPR regression models developed in this study. The predicted DCN decreased from the lighter end of the distillation cuts to the heavier end of the distillation cuts and the predicted RON increased from the lighter end of the distillation cuts to the heavier end of the distillation cuts.

When investigating the relationship between NO and the chemical functional groups it was found that there was a significant interaction between NO and the $(CH_2)_n$ functional group. When 200 ppm of NO was added to the charge air of the IQT and the DCN values of the TRF mixtures were measured it was found that increase in ignition propensity of the TRF mixtures, before and after NO addition, was directly related to the mole fraction of the $(CH_2)_n$ functional group. The relatively high mole fraction of the $(CH_2)_n$ functional group in the lighter end of the distillation cuts of the ethanol free gasoline signifies that there may be an interaction between the $(CH_2)_n$ functional group

and the residual NO in the cylinder either by remaining exhaust gases from the previous cycle or from exhaust gas recirculation. It can be assumed that the interaction between the NO and the $(CH_2)_n$ functional group may cause ignition to occur in the cylinder before the prescribed time because of the evaporation of the lighter end of the ethanol free gasoline. The premature ignition in the cylinder may be the cause of engine knock and LSPI in more recent downsized engines. Further investigations into the interactions of NO with the chemical functional groups should be done so that the chemical mechanisms that involve NO can be well defined.

Although the amount of energy produced by renewable resources is growing, most of the energy consumed is produced by burning fossil fuels. For this reason, it is vitally important to maximize the efficiency and minimize the emissions of processes that produce energy by burning fossil fuels until renewable resources can produce a larger percentage of the world's energy needs. In this thesis QSPR regression models were developed based on the chemical functional group distribution of TRFs and used to predict the RON, MON, and DCN of fuels. The effects of NO on the ignition propensity of TRFs were investigated and it was found that the relationship between NO and the $(CH_2)_n$ chemical functional group is significant and may lead to inefficiencies in engine performance, such as knock or LSPI. The work done in this research may lead to a better understanding of the effects of NO on the ignition propensity of fuels and help to maximize engine performance so that the inefficiencies of current engines can be reduced.

REFERENCES

1. U.S. Energy Information Administration. *Renewable energy explained*. 2021, May 20; Available from: https://www.eia.gov/energyexplained/renewable-sources/.
2. U.S. Energy Information Administration. *U.S. Energy facts explained*. 2021, May 14; Available from: https://www.eia.gov/energyexplained/us-energy-facts/.
3. Abd-Alla, G.H., *Using exhaust gas recirculation in internal combustion engines: a review*. energy conversion and management, 2002. **43**(8): p. 1027-1042.
4. Lu, T. and C.K. Law, *Toward accommodating realistic fuel chemistry in large-scale computations.* Progress in Energy and Combustion Science, 2009. **35**(2): p. 192-215.
5. Dooley, S., et al., *A jet fuel surrogate formulated by real fuel properties.* Combustion and flame, 2010. **157**(12): p. 2333-2339.
6. Dooley, S., et al., *The experimental evaluation of a methodology for surrogate fuel formulation to emulate gas phase combustion kinetic phenomena.* Combustion and Flame, 2012. **159**(4): p. 1444-1466.
7. Won, S.H., et al., *Reconstruction of chemical structure of real fuel by surrogate formulation based upon combustion property targets.* Combustion and Flame, 2017. **183**: p. 39-49.
8. Yuan, H., et al., *Optimal octane number correlations for mixtures of toluene reference fuels (TRFs) and ethanol.* Fuel, 2017. **188**: p. 408-417.
9. Naser, N., S.M. Sarathy, and S.H. Chung, *Ignition delay time sensitivity in ignition quality tester (IQT) and its relation to octane sensitivity.* Fuel, 2018. **233**: p. 412-419.
10. Chemistry LibreTexts. *5.3 nuclear magnetic resonance (nmr) spectroscopy*. 2019 June 5; Available from: https://chem.libretexts.org/Courses/Purdue/Purdue%3A_Chem_26505%3A_Organic_Chemistry_I_(Lipton)/Chapter_5._Spectroscopy/5.3_Nuclear_Magnetic_Resonance_(NMR)_Spectroscopy.
11. Cai, L. and H. Pitsch, *Optimized chemical mechanism for combustion of gasoline surrogate fuels.* Combustion and flame, 2015. **162**(5): p. 1623-1637.
12. Lamoureux, N., et al., *Experimental and numerical study of the role of NCN in the prompt-NO formation in low pressure CH4/O-2/N-2 and C2H2/O-2/N-2 flames (vol 157, pg 1929, 2010).* Combustion and Flame, 2013. **160**(3): p. 745-746.
13. Pitz, W.J., et al., *Development of an experimental database and chemical kinetic models for surrogate gasoline fuels.* SAE Transactions, 2007: p. 195-216.
14. Carpenter, D., et al., *Evaluating ignition propensity of high cycloparaffinic content alternative jet fuel by a chemical functional group approach.* Combustion and Flame, 2021. **223**: p. 243-253.

APPENDIX A: NMR SPECTROSCOPY OF ETHANOL FREE GASOLINE DISTILLATION CUTS.

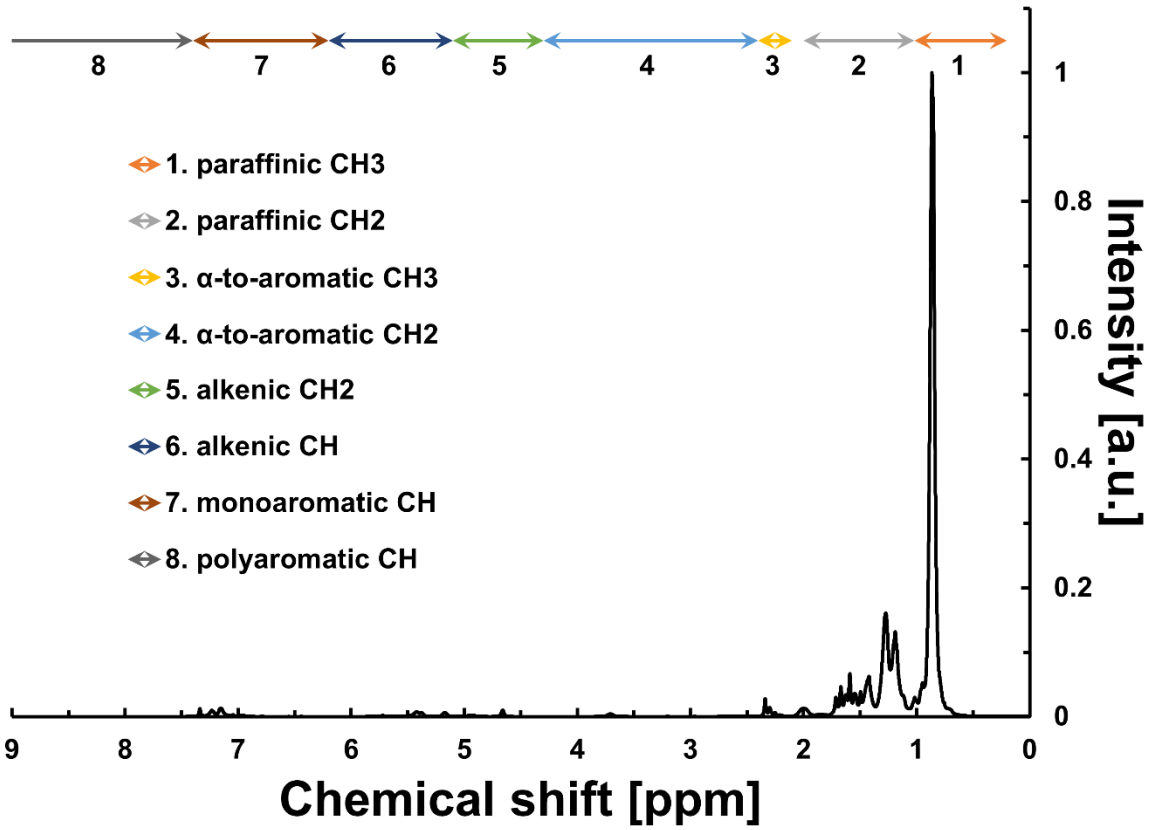

Figure A.1. ^{1}H NMR spectra for the first distillation cut of ethanol free gasoline.

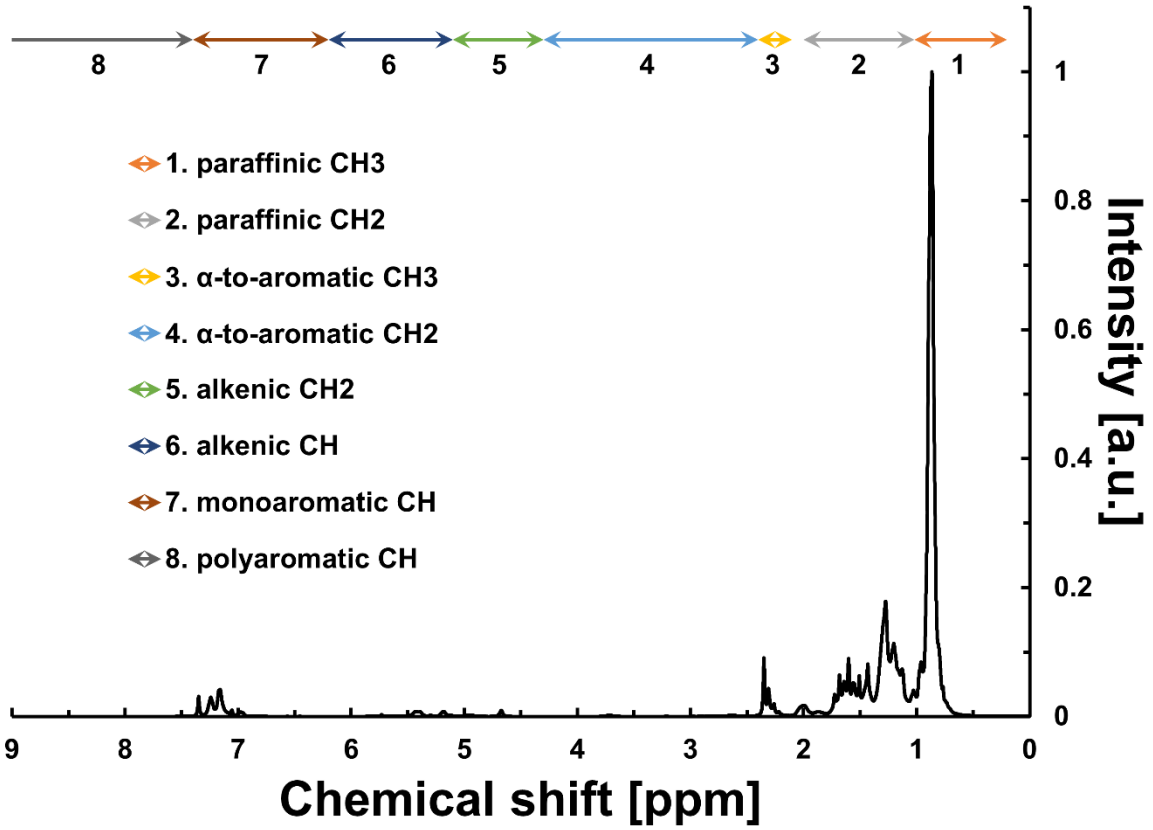

Figure A.2. ^{1}H NMR spectra for the second distillation cut of ethanol free gasoline.

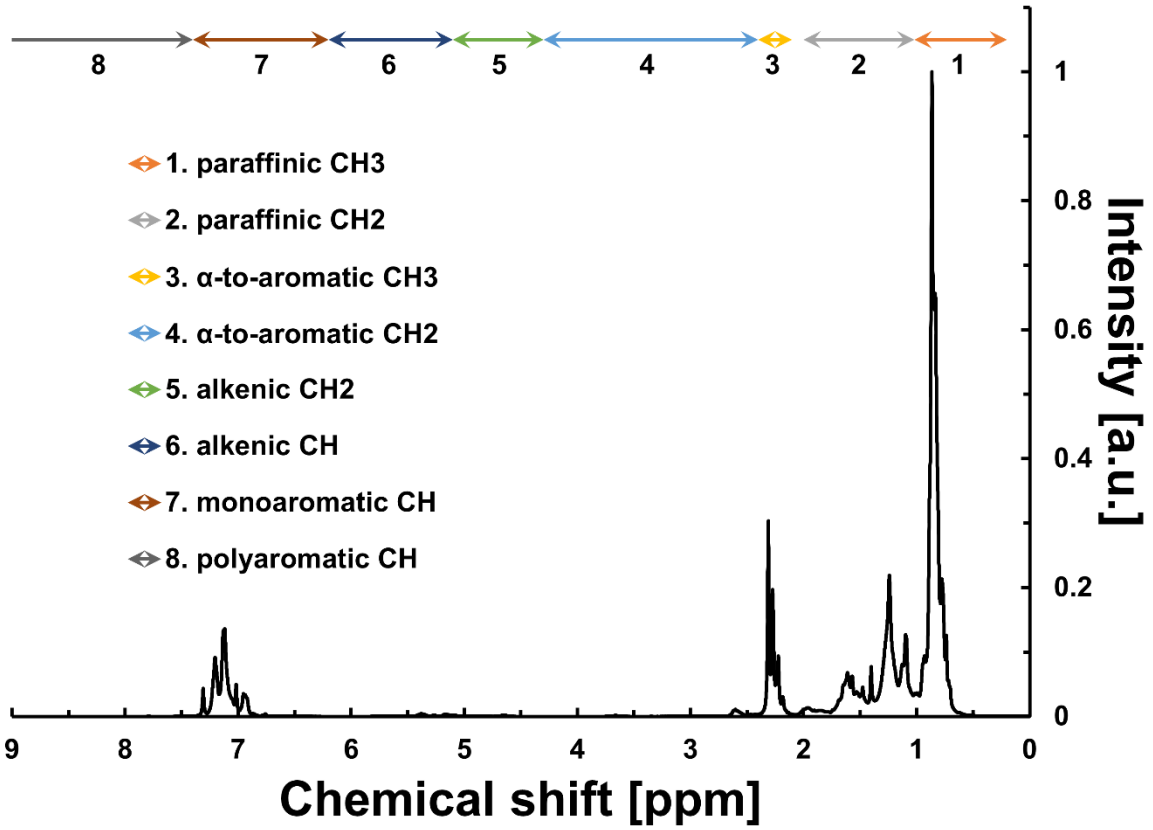

Figure A.3. ^{1}H NMR spectra for the third distillation cut of ethanol free gasoline.

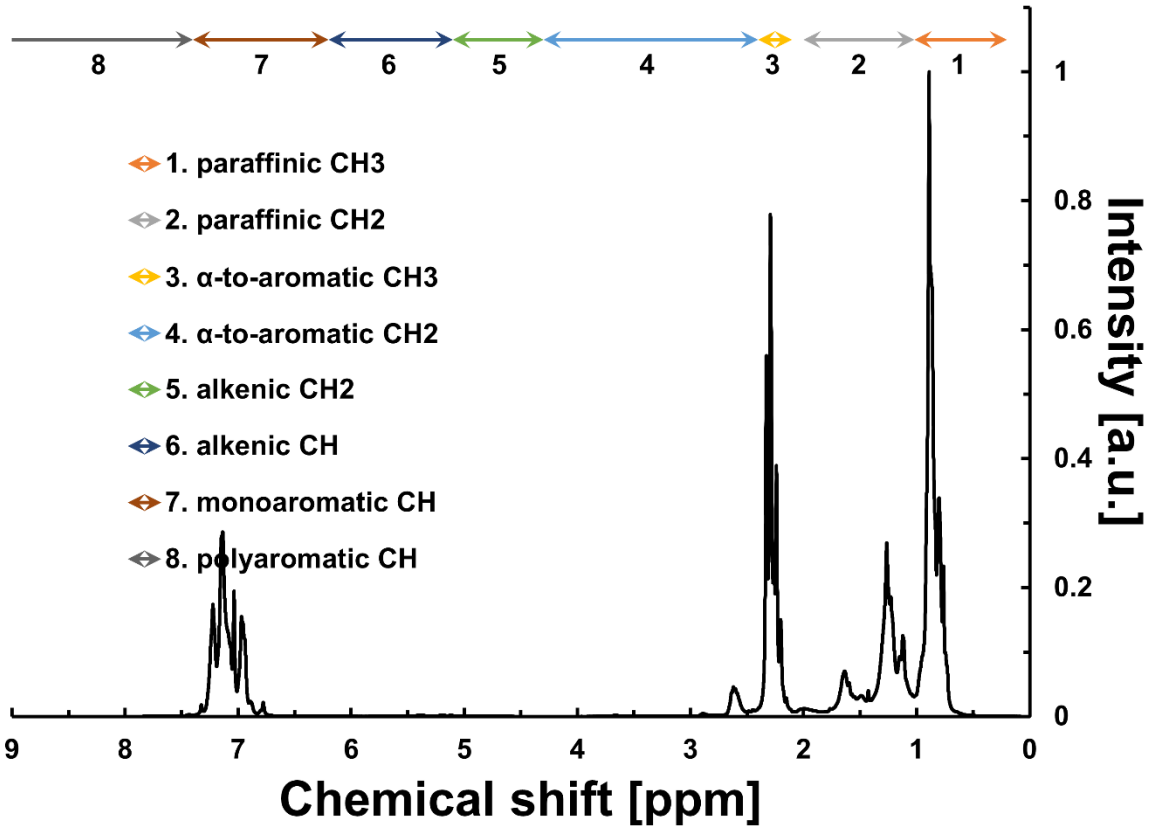

Figure A.4. ^{1}H NMR spectra for the fourth distillation cut of ethanol free gasoline.

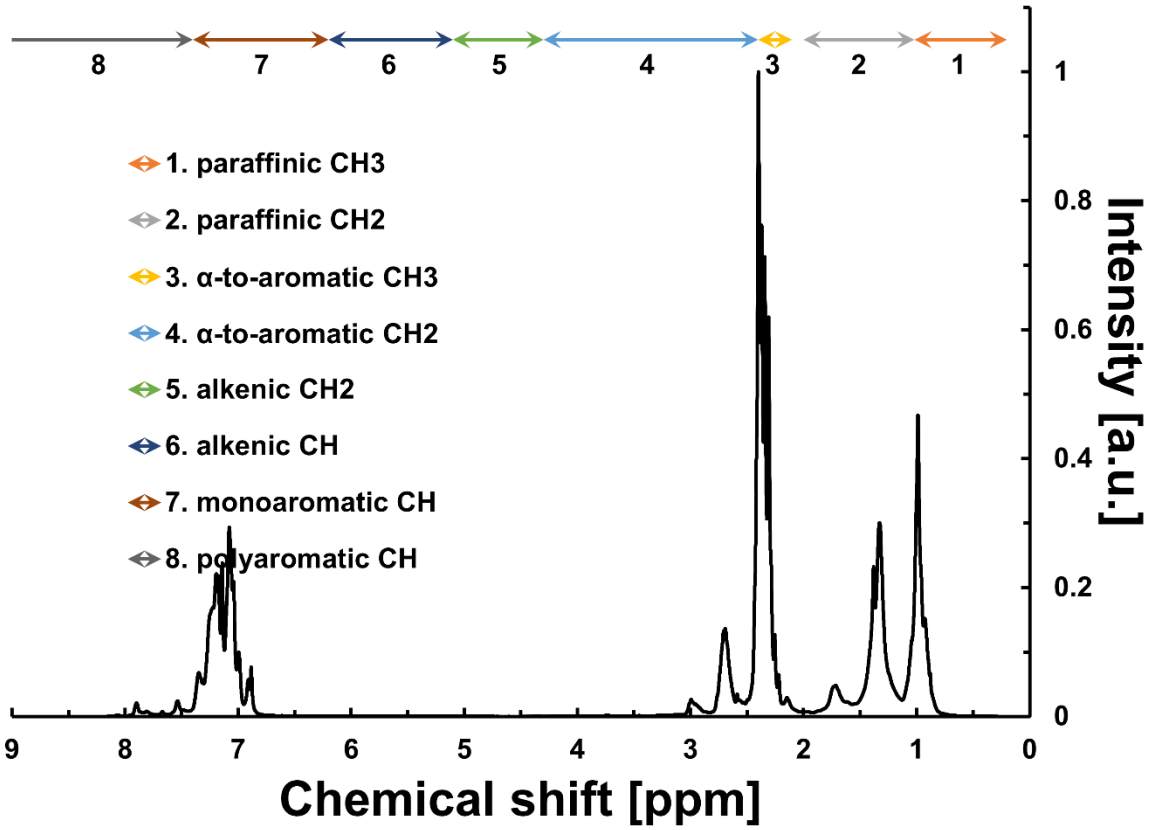

Figure A.5. ^{1}H NMR spectra for the fifth distillation cut of ethanol free gasoline.

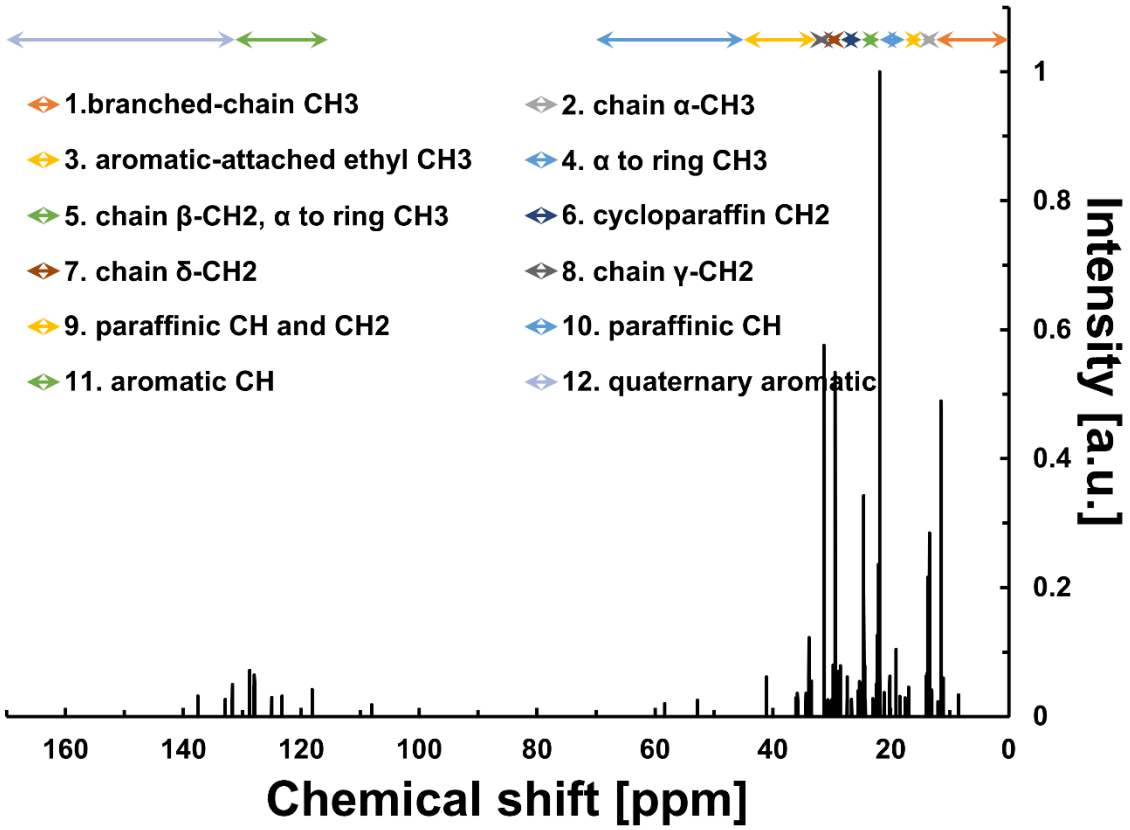

Figure A.6. ^{13}C NMR spectra for the first distillation cut of ethanol free gasoline.

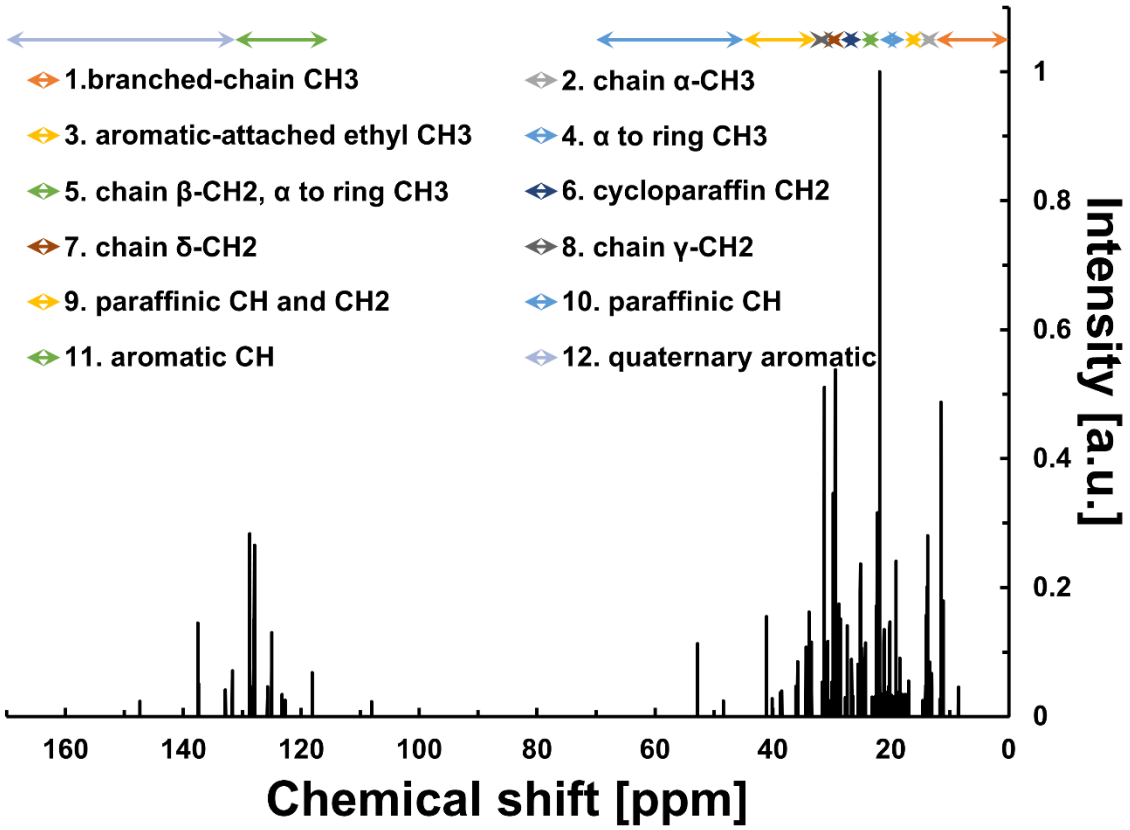

Figure A.7. ^{13}C NMR spectra for the second distillation cut of ethanol free gasoline.

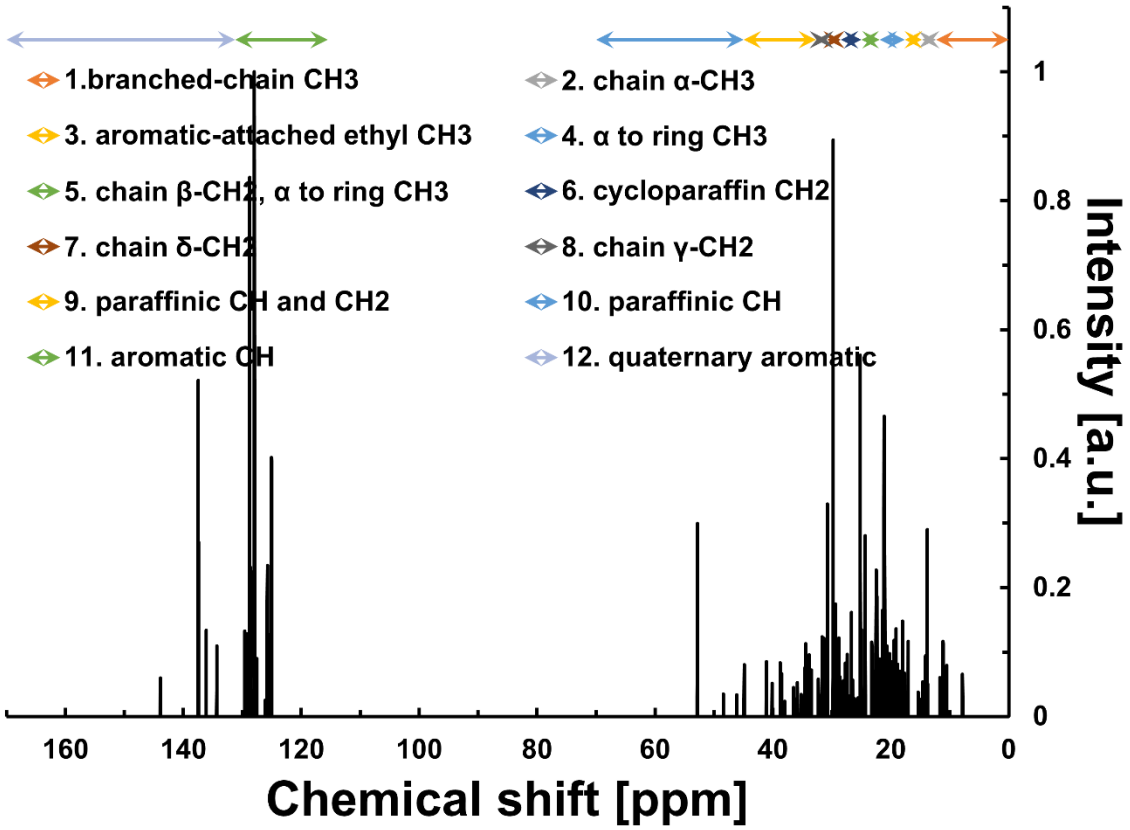

Figure A.8. ^{13}C NMR spectra for the third distillation cut of ethanol free gasoline.

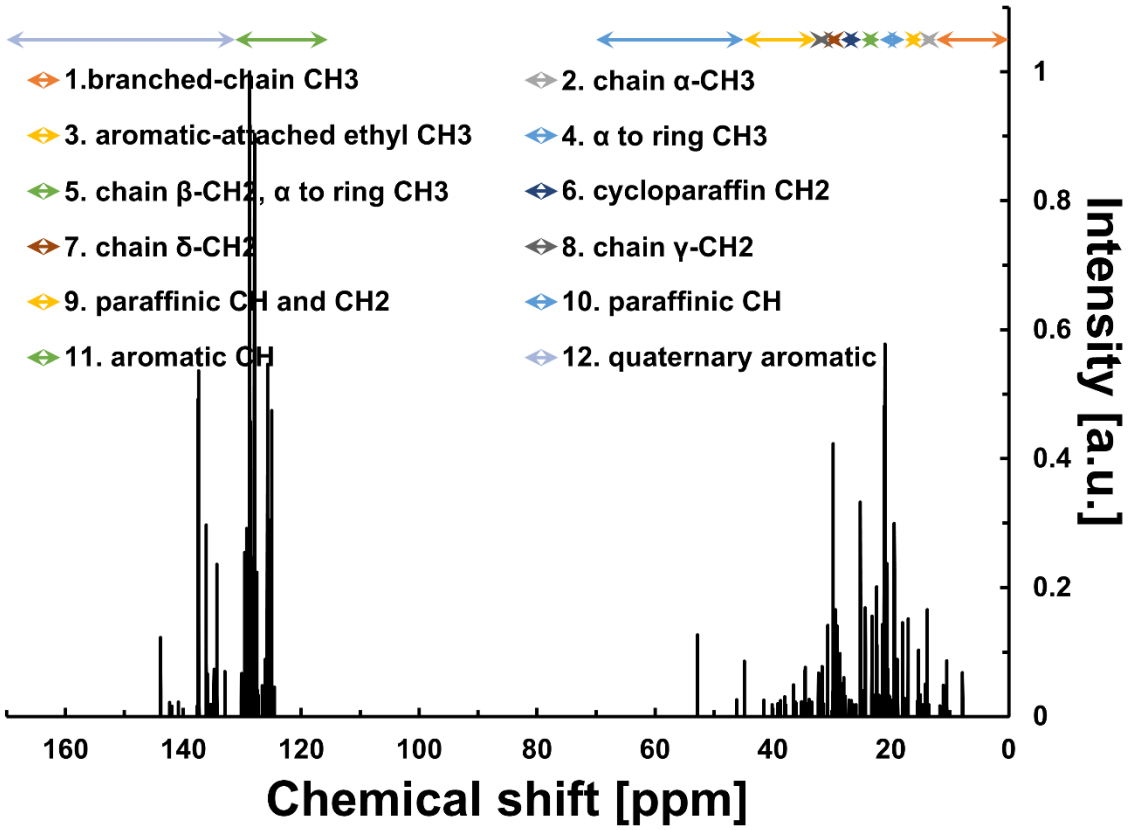

Figure A.9. ^{13}C NMR spectra for the fourth distillation cut of ethanol free gasoline.

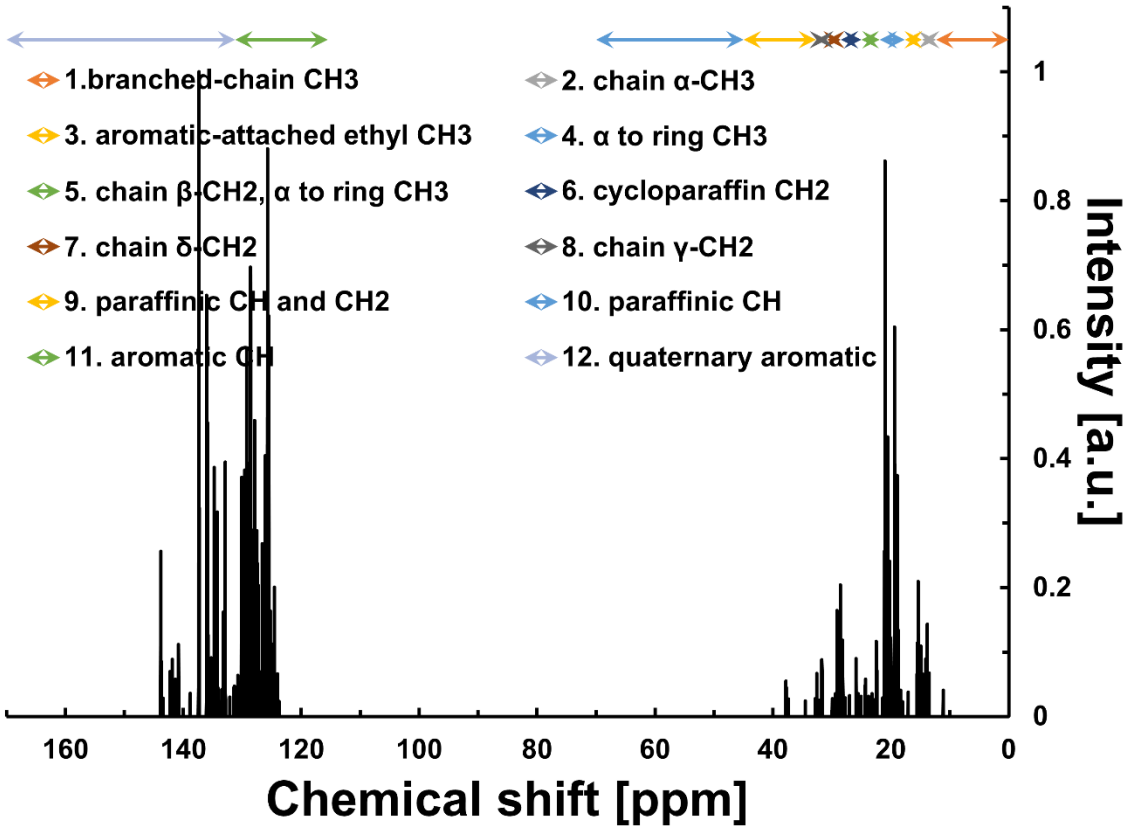

Figure A.10. ^{13}C NMR spectra for the fifth distillation cut of ethanol free gasoline.